ADVANCED MATERIALS INTERFACES
www.advmatinterfaces.de

A Route Towards Sustainability Through Engineered Polymeric Interfaces

*B. Reeja-Jayan, Peter Kovacik, Rong Yang, Hossein Sojoudi, Asli Ugur, Do Han Kim, Christy D. Petruczok, Xiaoxue Wang, Andong Liu, and Karen K. Gleason**

Chemical vapor deposition (CVD) of polymer films represent the marriage of two of the most important technological innovations of the modern age. CVD as a mature technology for growing inorganic thin films is already a workhorse technology of the microfabrication industry and easily scalable from bench to plant. The low cost, mechanical flexibility, and varied functionality offered by polymer thin films make them attractive for both macro and micro scale applications. This review article focuses on two energy and resource efficient CVD polymerization methods, initiated Chemical Vapor Deposition (iCVD) and oxidative Chemical Vapor Deposition (oCVD). These solvent-free, substrate independent techniques engineer multi-scale, multi-functional and conformal polymer thin film surfaces and interfaces for applications that can address the main sustainability challenges faced by the world today.

1. Introduction

In 2012, the General Assembly of the United Nations adopted a resolution on sustainability, entitling it "The Future We Want." This document highlighted the hallmarks of sustainable development, including access to potable water, adequate nutrition, and quality medical care. In addition, a sustainable world would be powered by clean energy sources, and its inhabitants would breathe unpolluted air.[1] All of these attributes are necessary for a successful, sustainable future; moreover, it is important to consider that these building blocks of sustainability do not exist in isolation, but are linked by complex relationships or "interfaces." A primary example is the link between energy sources, air pollution, and human health.[2,3] Another notable relationship exists between clean water and energy, often referred to as the "water-energy" nexus. Water is an essential component of the technical processes used to extract or harness energy; in return, the process of obtaining clean water is also highly energy-intensive.[4–6]

Energy-efficient Chemical Vapor Deposition (CVD) techniques can play an essential role in addressing many sustainability concerns. CVD processes enable engineering of extraordinary thin film interfaces, which can be integrated into a variety of applications, including clean energy technologies, high-efficiency techniques for extracting clean water, and low-power sensors. In CVD processes, vapor-phase precursors are introduced into a vacuum chamber. The precursors react on a surface, generating solid thin films. CVD methods have several distinct attributes. Film properties are easily tuned by adjusting the flow rate and composition of the feed vapors. In addition, the vapor-phase reactants readily diffuse into pores and other small features, resulting in "conformal" coatings with nanoscale uniformity. CVD processes have also been widely commercialized, particularly for depositing inorganic thin films for integrated circuit fabrication. The comparatively recent development of polymer CVD techniques has enabled users to harness the desirable qualities of CVD while fabricating flexible and responsive materials with a wide range of organic chemical functionalities.[7]

Functional polymer CVD interfaces have been integrated into several applications that directly address sustainability concerns (**Figure 1**). CVD polymer films can be used as thermal coatings to reduce energy consumption (Figure 1a).[8] Devices fabricated using CVD techniques also provide low-cost means of delivering therapeutic agents (Figure 1b).[9] CVD polymers can uniformly encapsulate particles of pharmaceutical and crop protection compounds,[10–12] ensuring efficient release of these materials with minimal waste (Figure 1c). Functional membranes coated with CVD polymers provide a simple and efficient route to extract microalgal intracellular biomass for cost-effective biodiesel production.[13] Low-power CVD polymer-based sensors provide sustainable ways to monitor humidity levels, detect hazardous pathogens in food, and alert citizens about toxic air pollutants (Figures 1d–f).[14–16] The use of polymer CVD methods provides additional benefits with regard to sustainability. While solution-phase processes can be used to develop chemistries for applications like those shown in Figure 1, all-dry CVD methods avoid the deleterious health, safety, and environmental concerns associated with solvent use. The lack of solvent is beneficial from an economic perspective and improves the capabilities of the coating process, as concerns about surface tension and dewetting effects and polymer-solvent miscibility are eliminated. Additionally, CVD methods are typically fast, highly efficient, one-step processes. Newer CVD techniques have been specifically designed to enable low-temperature deposition of polymer thin films. These attributes

B. Reeja-Jayan, P. Kovacik, R. Yang, H. Sojoudi, Asli Ugur, D. H. Kim, C. D. Petruczok, X. Wang, A. Liu, Prof. K. K. Gleason
Chemical Engineering
Massachusetts Institute of Technology
Cambridge, MA 01239–4307
E-mail: kkgleasn@mit.edu

DOI: 10.1002/admi.201400117

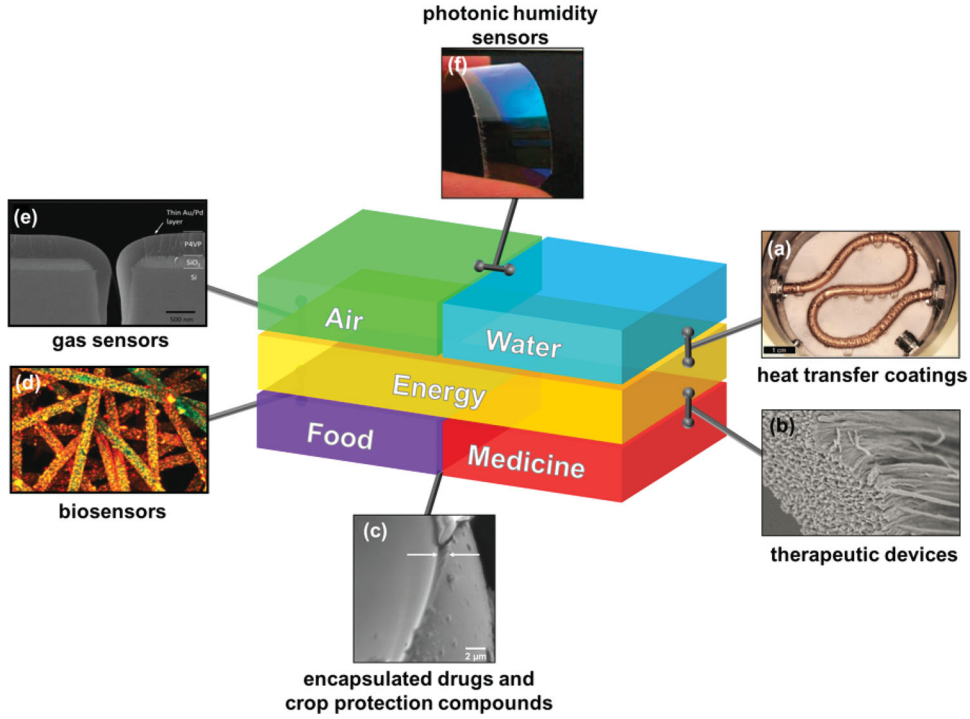

Figure 1. Key concerns interfacing the building blocks of sustainable development (air, water, energy, food, and medicine) are addressed with polymer chemical vapor deposition (CVD) interfaces and devices. (a) Highly cross-linked CVD fluoropolymer coatings promote dropwise condensation, reducing energy consumption for industrial processes.[8] (b) Polymer "microworm" devices fabricated via a low-energy CVD process are used to efficiently deliver therapeutic agents.[9] (c) CVD polymers uniformly coat particles and are used as an encapsulant for pharmaceutical and crop protection compounds.[10–12] (d) A functionalized, conducting CVD polymer is integrated into low-energy resistive biosensors for food pathogens.[15] (e) Hazardous chemicals are readily detected using low-power CVD polymer gas sensors.[16] (f) A flexible Bragg mirror is constructed from alternating CVD layers of polymer hydrogel and titania and used as a humidity sensor.[14] Insets (a)-(f) adapted with permission from.[8–10,14–16] Insets (a)-(f) reproduced with permission. (a) Copyright 2013, Wiley.[8] (b) Copyright 2011, National Academy of Sciences, USA.[9] (c) Copyright 2008, American Chemical Society.[10] (d) Copyright 2011, Wiley.[15] (e) Copyright 2010, Wiley.[16] (f) Copyright 2008, American Chemical Society.[14]

reduce energy use and operational costs as well as protect the integrity of polymer functional groups and the substrate.[17]

A variety of polymer CVD processes are in use today. The first of these techniques, parylene CVD, was initially demonstrated in 1947 and refined by Gorham in 1966.[18,19] Poly(p-xylylene) ("parylene") films are commonly synthesized by thermally cracking [2.2] paracyclophane to yield monomers that self-initiate polymerization on cooled substrates. The parylene CVD process has been heavily commercialized, and these materials have been implemented in variety of applications, including printed circuit boards and biomedical devices.[20,21] Polymer thin films have also been synthesized using Vapor Deposition Polymerization (VDP). In this process, two bifunctional monomers are co-evaporated and react through a condensation step-growth mechanism to form a polymer film.[22] In a variant of this method, Surface-Initiated VDP (SI-VDP), the vapor-phase monomers react with compatible functional groups on a substrate, generating a grafted film.[23] Molecular Layer Deposition (MLD) is a process in which two monomers are alternately introduced into a vacuum chamber under self-limiting reaction conditions. The MLD process yields ultra-thin and highly conformal films.[24] Another well-established CVD technique is Plasma-Enhanced Chemical Vapor Deposition (PECVD), in which monomer species are bombarded with charged species in the plasma, ultimately resulting in fragmentation and free radical polymerization through a complex series of reactions.[25,26] The resulting films are typically highly cross-linked and mechanically robust; however, the non-selective initiation can limit the retention of functional groups from the monomer, affecting the properties of the material.[26,27] This phenomenon can be avoided by using a technique with a selective initiation process, such as initiated Chemical Vapor Deposition (iCVD). In this method, monomer(s) and a thermally labile initiator flow into a vacuum reaction chamber, passing through an array of heated filaments. The thermal energy from the filaments generates initiator radicals, which react with adsorbed monomer on a cooled substrate, forming a polymer film.[28,29] In oxidative Chemical Vapor Deposition (oCVD), a volatile monomer and oxidant are introduced into the reaction chamber, and step-growth polymerization occurs on the cooled substrate.[30] A variant of this technique, Vapor Phase Polymerization (VPP), requires pre-application of the oxidant in the liquid phase followed by introduction of monomers in the vapor phase.[31] One hallmark of the iCVD and oCVD processes is their benign reaction conditions. In the iCVD technique, the temperature of the filament is low enough to prevent damage of the monomer species during polymerization.[17,32] This low-temperature process is extremely efficient, with an energy density one order of magnitude of lower than that of PECVD.[33] In both the iCVD and oCVD processes, the substrate is maintained at or near

room temperature, preserving the integrity of the polymer films, reducing energy usage, and facilitating film deposition on delicate substrates, including paper and fabric.[17,32]

This review discusses the use of energy-efficient chemical vapor deposition (CVD) techniques to engineer extraordinary polymer thin film surfaces and interfaces for applications addressing key sustainability issues. In particular, we emphasize the iCVD and oCVD techniques developed in our laboratory. We begin with an overview of these methods, followed by an analysis of the scalability of these processes to address energy usage and economic concerns. Next, the integration of iCVD and oCVD polymer interfaces into sustainable applications, including photovoltaic and electrochemical energy harnessing, electrochemical energy storage, water desalination, enhancing heat exchange, and air, food quality monitoring is discussed. We conclude with commentary on the future prospects of these enabling technologies to engineer pathways that lead to achieving the goal of sustainability.

1.2. Mechanistic of Surface/Interface Modifications

1.2.1. Classification of Polymer CVD Techniques by Polymerization Mechanism

Chain Growth Polymerization: The method of initiated chemical vapor deposition (iCVD) is the vapor-phase analog of solution-phase free radical polymerization.[34] Initiating species (e.g., tert-butyl peroxide) and chain growth monomers (e.g., acrylates, methacrylates, styrenes, vinylpyrrolidone, divinylbenzene) in the vapor phase are delivered to the surface of a temperature controlled substrate, placed inside a custom-built vacuum chamber (reactor). As depicted in **Figure 2**a, resistively heated filaments crack the initiator molecules to form free radicals, which subsequently react with the monomers adsorbed on the cooled substrate surface, resulting in simultaneous polymerization and thin film growth on the substrate.[7,32,35] Reactor pressure, reactant flow rates, substrate and filament temperatures are key parameters used to control film growth.[29,36] The in situ monitoring of film thickness during deposition can be achieved by using either laser interferometry through a reactor window or by quartz crystal micro-balances (QCMs), facilitating process development and allowing precise control of film thickness over a wide range (**Figure 3**a-b).

iCVD can grow films from virtually any vinyl monomer that can generate sufficient vapor pressure to be delivered into the reactor, and is particularly desirable for the growth of homopolymers, co-polymers,and graded polymer films that are difficult to synthesize by solution-phase methods. The relatively modest temperatures (<300 °C) of the filaments ensure that the monomer molecules remain chemically intact, resulting in full retention of organic functional groups (e.g.,-OH, -COOH,-C = O, -NH_2) in the iCVD grown polymer films. In plasma-based polymer CVD techniques (e.g., PECVD), the highly energetic species present in the plasma collide with and fragment the monomer, leading to reduced retention of functional groups.[17,41] As discussed in the following sections, the full retention of organic functionality in iCVD grown polymer films is critical for their myriad applications like tuning surface energy, generating responsive surfaces, and engineering polymer interfaces tethered to cells, tissues, and nanoparticles.

Step Growth Polymerization: Oxidative chemical vapor deposition (oCVD) mirrors solution based oxidative polymerization in the vapor phase.[42] While iCVD typically synthesizes insulating/dielectric polymer films, oCVD enables the vapor-phase step-growth polymerization of thin films of electrically conducting polymers (e.g., poly(ethylenedioxythiophene) (PEDOT), polypyrrole (PPy), poly(3-thiopheneacetic acid) (PTAA)). Instead of initiating radicals, a solid-state oxidant (e.g $FeCl_3$) is sublimed by heating to ~ 350 °C and spontaneously reacts with the heated monomer vapors that flow into the oCVD reactor (Figure 2b), Adsorption and polymerization happen simultaneously on the surface of a temperature controlled substrate placed upside down over the oxidant crucible.[41,43] Both work function and conductivity of the polymer films can be tailored by varying the substrate temperature, enabling a host of conducting polymer films for applications in photovoltaics and energy storage. The all vapor nature of oCVD makes it suitable for growing conducting polymer films on environmentally friendly substrates like paper. Indeed, oCVD grown PEDOT films demonstrate excellent conductivities (>2000 S/cm), comparable to VPP and solution-cast films.[44] Furthermore, difficulties associated with film dewetting and substrate degradation by solvents can be completely avoided in oCVD, enabling highly conductive PEDOT films grown by oCVD to be easily integrated with a variety of unconventional surfaces (e.g., graphene).[45]

1.2.2. Engineering "Extraordinary" Polymer Surfaces and Interfaces

In both iCVD and oCVD, the rate of polymerization and film growth depends on the amount of monomer adsorbed onto the substrate surface. Maintaining substrates at lower temperatures promote adsorption of the monomer, leading to fast film deposition rates (exceeding 100 nm/min) and high molecular weight polymer chains.[46] The surface concentration of monomer at a given temperature can be directly related to the dimensionless ratio (P_M/P_{sat}), defined between monomer partial pressure (P_M) and saturation pressure of the monomer at the substrate surface (P_{sat}).[29] For most iCVD processes, film growth is carried out at P_M/P_{sat} values of 0.3 to 0.7. Operating within this range concentrates monomer species to liquid-like concentrations on the substrate surface and promotes uniform film growth without leading to undesirable liquid-phase condensation (P_M/P_{sat} ~ 1). Employing P_M/P_{sat} as a figure of merit along with real-time monitoring of film growth thus facilitates the growth of polymer films of varying thicknesses ranging from nanoscale antifouling coatings on reverse osmosis membranes (Figure 3a),[37] to impressively thick macroscale films (Figure 3b).[38] This remarkable ability for multiscale thickness control is one of the strongest features of polymer film growth by iCVD and oCVD, when compared to solution-based techniques.

iCVD and oCVD film growth is compatible with traditional micro fabrication techniques, and can be patterned by lithographic techniques, microcontact printing, and by using shadow masks or vapor printing. Patterning provides a route to tailor polymer film surfaces both chemically and topographically. In

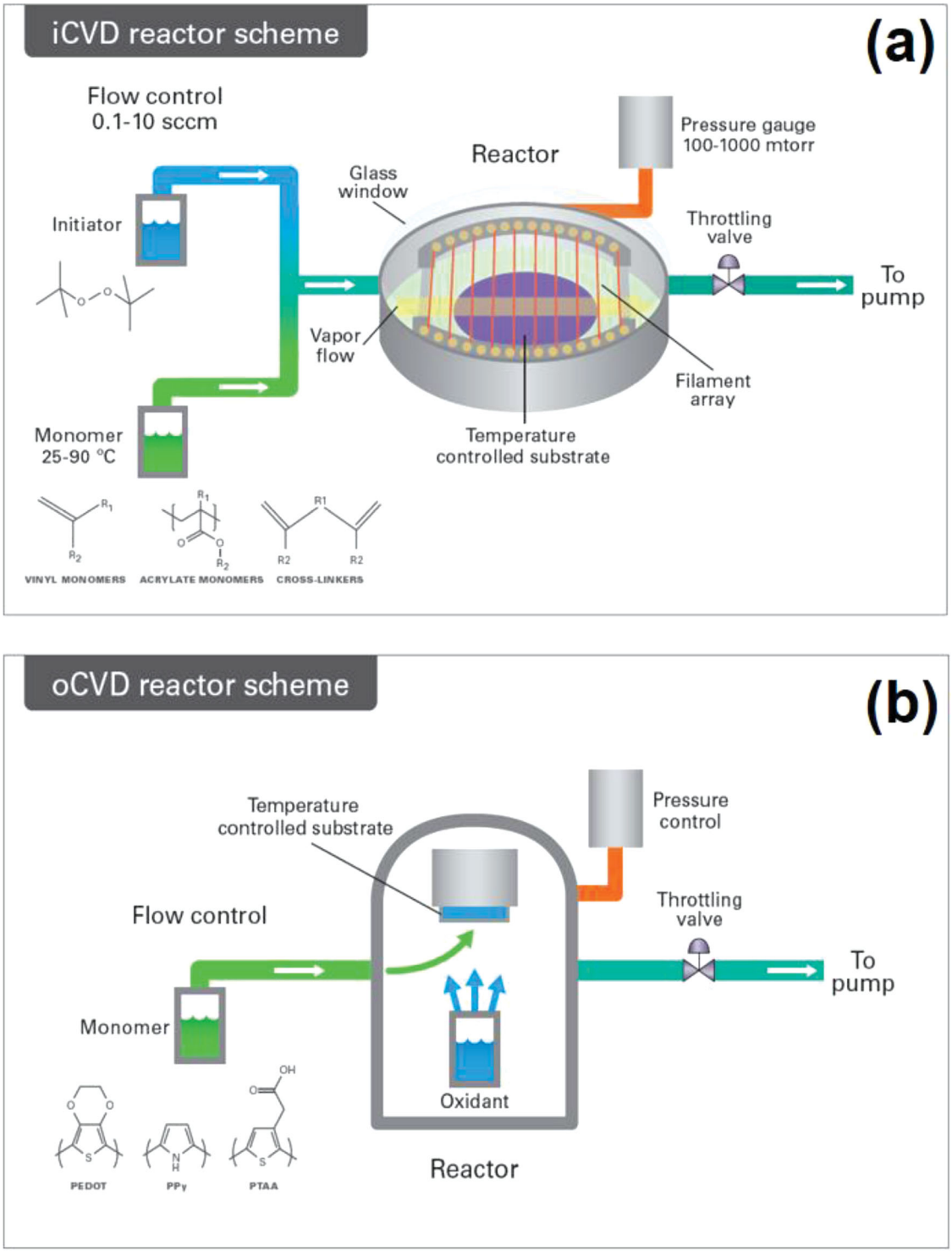

Figure 2. Schematic of (a) iCVD reactor, (b) oCVD reactor.

Figure 3c, a TEM grid is used as shadow mask to pattern multifunctional iCVD films comprising of hydrophobic wells of poly(perfluorodecylacrylate) (pPFA) surrounded by hydrophilic poly(hydroxyethylmethacrylate) (pHEMA) regions.[39] These microwell structures can spatially confine water droplets to the hydrophilic regions, creating durable hydrophobic water shedding surfaces for water desalination and power generation. When such patterned films are immersed in water, the hydrophilic pHEMA regions selectively swell, varying the depth of the microwells, suggesting potential applications for such patterned

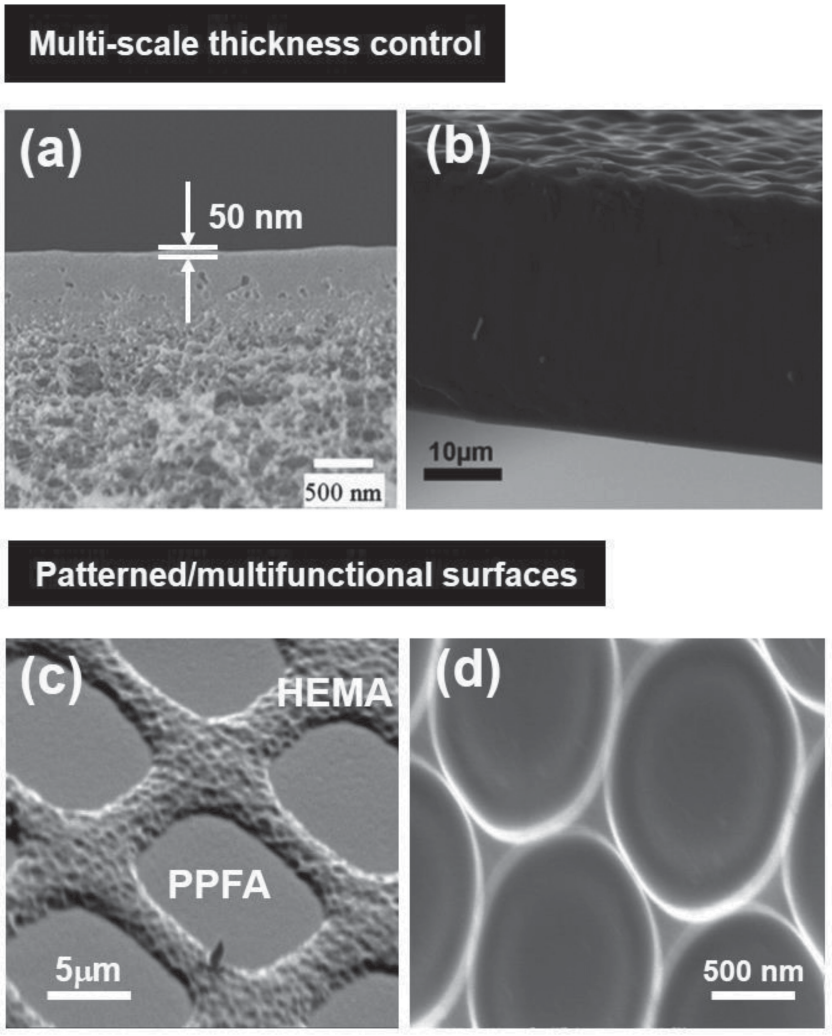

Figure 3. Multiscale thickness control. (a) Ultra-thin iCVD grown copolymer films of amphiphilic p(HEMA-co-PFDA) on reverse osmosis (RO) membranes.[37] (b) 30 micrometer thick poly(glycidyl methacrylate) (pGMA) films made possible by fast (>300 nm/min) deposition rates in iCVD.[38] (c) iCVD dual-patterned multifunctional surface with hydrophobic pPFDA in the squares and hydrophilic pHEMA in the surrounding matrix.[39] (d) Colloidally patterned oCVD PEDOT nanobowls. Roughness of these surfaces can be tuned by changing the oxidant used in oCVD.[40] (a) Reproduced with permission.[37] Copyright 2013, Elsevier. (b) Reproduced with permission.[38] Copyright 2012, American Chemical Society. (c) Reproduced with permission.[39] Copyright 2010, Wiley. (d) Reproduced with permission.[40] Copyright 2010, Royal Society of Chemistry.

responsive surfaces in sensing. As the thickness of the growing polymer film can be monitored in real-time, the height of the two polymer regions can be precisely controlled to produce various topographic features, adding to the multifunctional capabilities of these films. In another example (Figure 3d), colloidal polystyrene (PS) beads were used as template to pattern oCVD PEDOT films as nanobowls, while preserving the high electrical conductivity of the bulk polymer.[40] The ability to create a covalently bonded (grafted) interface between the PEDOT and the underlying substrate is the key to realizing this simple, one-step process that can simultaneously pattern the PEDOT surface for applications like plasmonics, and functionalize the PEDOT surface to attach biomolecules. The high surface area of these conductive PEDOT nanostructures further makes them attractive as electrodes for supercapacitors and lithium-ion batteries.

In both iCVD and oCVD polymerization, reactants arrive at the substrate surface through non-directional vapor phase diffusion. There is only a limited probability that these reactants will "stick" to the surface during any single collision event. Unlike solution processing, vapor-phase deposition does not suffer from surface tension and dewetting effects, which lead to non-uniform film thicknesses. Consequently, under appropriate deposition conditions, iCVD and oCVD grown polymer films are highly conformal i.e., as these films grow, they uniformly trace the contours or geometric features present on the substrates (**Figure 4**a). Quantitative models for understanding conformal coverage by iCVD films have been reported by Baxamula et al.[47] Briefly, both the aspect ratio of the structures being coated and the P_M/P_{sat} ratio determine conformal coverage. For a given aspect ratio, low P_M/P_{sat} ratios result in excellent conformality (Figure 4a). As P_M/P_{sat} ratios increase towards super-saturated conditions, the films tend to become less conformal and non-uniform (Figure 4b). Figures 4c–e depicts examples of multi-scale conformal coverage by iCVD films on non-planar surfaces with nano and micro-scale features. In Figure 4d, conformal pH responsive (poly(methacrylic acid-co-ethylene glycol diacrylate) (p(MAA-co-EGDA)) hydrogel coatings "shrink-wrap" vertically aligned carbon nanotubes, significantly enhancing the wettability of the nanotube surface for *in vivo* and *in vitro* sensing.[48] Figure 4e depicts smooth, thin coatings of (poly(methylmethacrylate) (PMMA)) on the surfaces of wool fabrics, which protects dyed wool textiles against light induced degradation.[49]

The ability to engineer functional polymer surfaces with tunable nanostructure, nanoporosity and high interfacial area is critical for photovoltaics, lithium ion batteries, supercapacitors and sensors. In the example depicted in **Figure 5**a, oCVD using $CuCl_2$ oxidant demonstrated systematic control over both porosity and surface morphology of PEDOT films, simply by varying the substrate temperature.[50] Combining such nanoscale surface roughness with the microscale texture of naturally rough substrates like paper or textile fabrics can tune the surface energy of these substrates leading to superhydrophobic surfaces that emulate the "lotus leaf" effect (Figure 5b).[51] There is currently a growing number of "green" applications for such surfaces from design of self-cleaning textiles to de-icing of power transmission lines. As both iCVD and oCVD coatings are conformal, the underlying roughness of substrates gets invariably transferred to the growing films. The

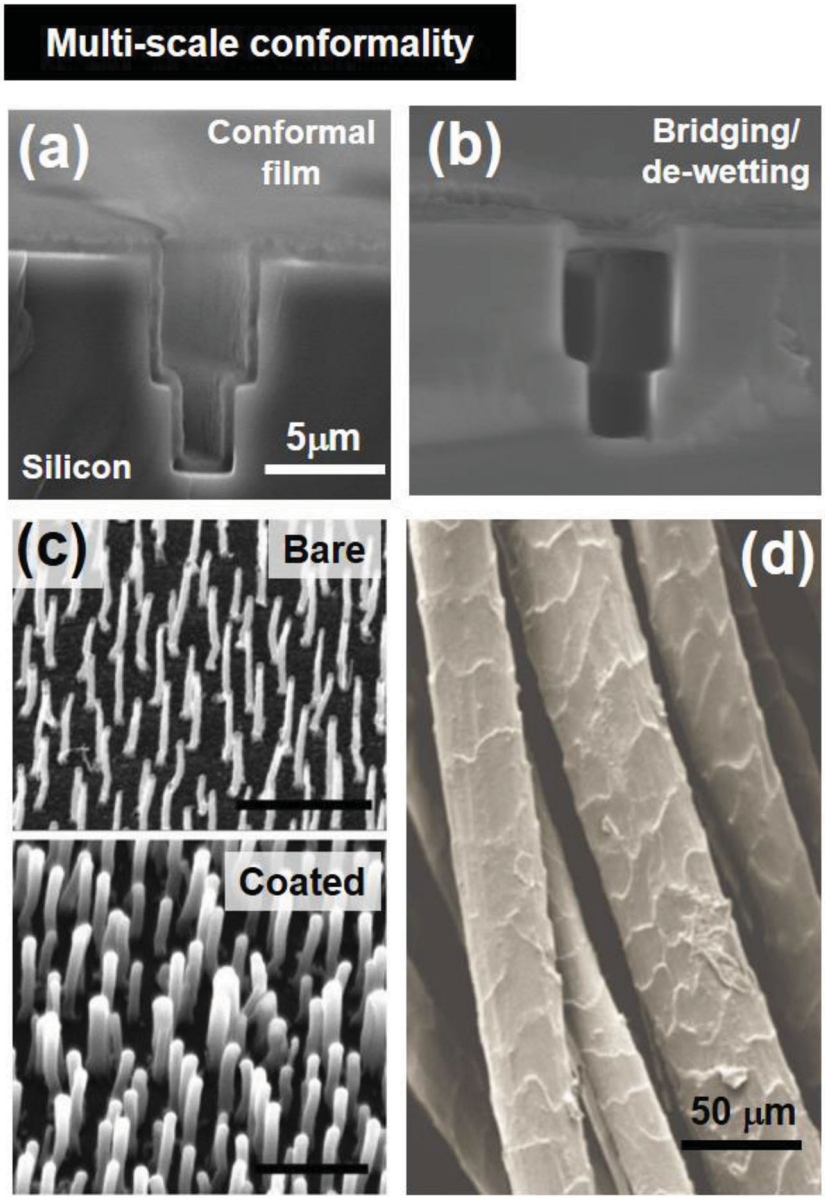

Figure 4. Multiscale conformality of iCVD films. (a) Perfectly conformal polymer film demonstrates uniform thickness along a microtrench cut into silicon wafer. (b) Deposition under super-saturated conditions results in liquid phase wetting and non-conformal "bridging" film across the trench. (c) SEM images of vertically aligned carbon nanotubes before (top) and after (bottom) conformal coating with 50 nm layer of p(MAA-co-EGDA) by iCVD. Scale bar is 2 μm.[48] (d) Wool fibers conformally coated with iCVD PMMA. The structure of the underlying fiber surface is visible after coating demonstrating the delicate nature of the iCVD process.[49] (c) Reproduced with permission.[48] Copyright 2011, Royal Society of Chemistry. (d) Reproduced with permission.[49] Copyright 2013, American Chemical Society.

example in Figure 5c demonstrates carbon nanotubes serving as templates for the nucleation and growth of crystalline polytetrafluoroethylene (PTFE), resulting in the aggregation of these crystals into a nano-hybrid "shish-kebab" or "string of pearls" morphology.[52] Given the technological relevance of many polymers referenced here (e.g., PTFE, PEDOT), the ability of iCVD and oCVD to simultaneously control both the surface chemistry and the surface morphology of polymer films is significant.

While previous examples focused on all solid thin film interfaces, the example in Figure 5d uses iCVD to grow stable polymer films on the surface of a drop of ionic liquid (*i.e* at the liquid vapor interface). By varying the surface energy and solubility of the deposited polymer, either continuous films or particles can be deposited.[53] Alternatively, depending on the solubility of the monomer in the liquid, the film can be deposited at the liquid-vapor interface or inside the liquid drop; a feat impossible by solution casting.[54] High molecular weight polymer films grown inside the liquid drop can even form solid-like gels, which can potentially be used as membranes in fuel cells and in gas separation processes.

Finally, incorporating functional groups onto the surface of both iCVD and oCVD grown polymer films can easily attach nanoparticles, quantum dots and even biological matter to these films. **Figure 6**a depicts examples for 4-aminothiophenol,[55] azide,[56] and amine-peptide[57] linker molecules that respectively enable such hybrid polymer-inorganic and polymer-biomolecule interfaces with remarkable chemical and biological specificity. The ability to engineer the interface between the substrate and the growing polymer film is yet another important capability, particularly for fabricating thin film devices. In iCVD, functionalizing the surface of the substrate with vinyl groups creates radical sites on the surface that covalently connect (graft) the substrate to the polymer (Figure 6b).[56,58,59] Such grafted films are strongly adhered to the underlying substrate, and cannot be damaged by repeated sonication or other mechanical delamination tests. Another oCVD approach uses aromatic groups present on the surface of certain substrates (e.g., polystyrene (PS), polyethylene terephlate (PET)) to create radical sites directly on the substrate using the Friedel Crafts reaction between the aromatic group and the oxidant (PEDOT nanobowl example in Figure 3d).[40,60] The iCVD equivalent of this linker free grafting approach is to create vinyl groups on the substrate surface, which can then be used to graft an iCVD film.[61] In an example of this technique, Si-H bonds present on a native oxide stripped silicon surface were abstracted by initiator radicals to form reactive sites at which vinyl groups can be anchored. Once grafted to the substrate surface, the iCVD and oCVD polymer films can be patterned (Figure 3d) or wrinkled,[62] to create topographic features for plasmonics, or even reduce surface dangling bonds in crystalline silicon solar cells.

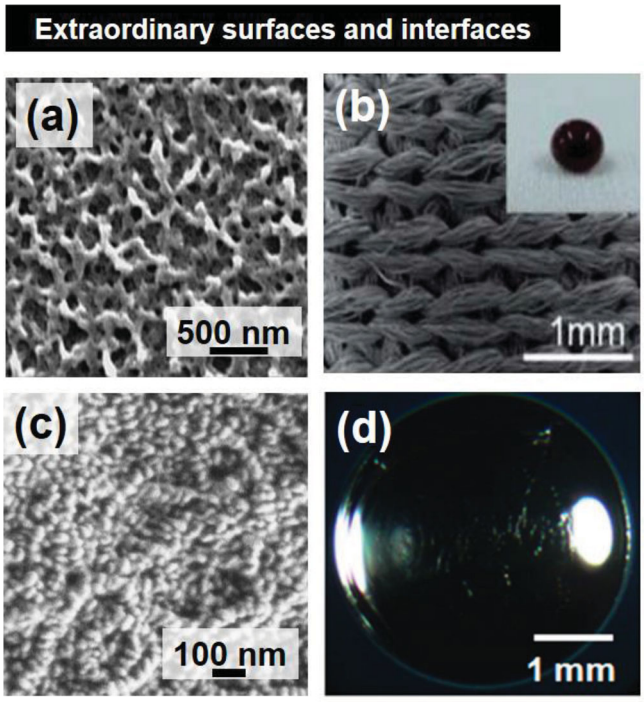

Figure 5. (a) Nanoporous PEDOT films with basalt-like surface morphology obtained using $CuCl_2$ as oxidant in oCVD.[50] (b) Super-hydrophobic polyester fabric with stacked polytetravinytetramethycyclotetrasiloxane-polyfluorodecylacrylate (p(V_4D_4-PFDA)) coating deposited by iCVD. Inset depicts a drop of aqueous blue ink on the coated surface with contact angle exceeding 150°.[51] (c) "Shish-kebab" surface morphology of 40 nm thick iCVD PTFE film grown over carbon nanotube templates. PTFE crystals nucleate onto the nanotube, organize into aggregates and finally grow along the nanotube axis.[52] (d) iCVD grown continuous PFDA film on a drop of [emim][BF_4] ionic liquid. It is energetically favorable for low surface tensions films like PFDA to spread over the liquid surface.[53,54] (a) Reproduced with permission.[50] Copyright 2008, American Chemical Society. (b) Reproduced with permission.[51] Copyright 2012, Royal Society of Chemistry. (c) Reproduced with permission.[52] Copyright 2012, Wiley. (d) Reproduced with permission.[53]

For details on the physical mechanisms governing polymer film growth and interface engineering in iCVD and oCVD, the interested reader is directed to a previously published review article.[32] The succeeding sections of this review will focus on various applications for sustainable use of energy, water and other natural resources, made possible by the amazing properties of iCVD and oCVD polymers mentioned in this section. **Table 1** summarizes these distinguishing characteristics of iCVD and oCVD that can address the challenges of designing materials and techniques for an environmentally-benign, economically viable future.

1.3. Reactor Design Principles

As previously discussed, basic principles of polymer CVD are relatively simple and so are the technical requirements for designing the CVD reactor. Whether the substrate is already pre-treated with initiator or oxidant, or one of these is introduced as a vapor flow to subsequently mix with the monomer, the reactor architecture can be designed with great flexibility as desired for the particular application. For example, Hassan et al. have demonstrated an elegant solution for encapsulation of wool fabrics by UV-protecting poly(methyl methacrylate), PMMA.[49] **Figure 7**a illustrates a simple CVD reactor which consists purely of an evacuated glass vessel heated by the outer glycerin bath. A dish with MMA monomer is placed at the bottom of the vessel just below the wool substrate. Heated MMA evaporates onto the fabric where it reacts with the pre-coated initiator and subsequently polymerizes, leading to conformal coating of the wool fibers with PMMA (Figure 4d). As shown previously in Figure 2, the oCVD and iCVD methods are principally similar, and allow for adjustment of the oxidant or the initiator flow rates, thus enhancing the ability to control the polymer film growth.[28–30]

The key process parameters, namely chamber pressure, reactant flow rate, and substrate temperature, each play an interdependent role in determining the growth rate of the polymer film and its chemical and morphological properties. A detailed discussion on these relations can be found in our previous reviews.[17,35] As regards the technical values, the reactants are usually introduced as vapors at flow rates on the order of ~0.1 to ~10 sccm into a chamber operating under medium vacuum ~0.1–1 torr. The substrate temperatures range between 20 – 80 °C for iCVD and 20 – 200 °C for oCVD. To note, these are standard conditions for the lab-sized oCVD and iCVD reactors (~1 cf and ~0.5 cf in volume, respectively) used in most of our previous studies. In order to achieve uniformity of the film properties, substrate heating, flow mixing, and flow patterns within the reactor should all be as uniform as possible. Reactors with a degree of symmetry are therefore desired.

1.4. Reactor Scale-up and Commercialization

The in-situ process parameters are necessarily entangled with the geometrical parameters of the reactor itself. Sufficient consideration should hence be given to fluid mechanics, mass and heat transport, as well as the reaction kinetics – especially when designing a new CVD reactor, scaling up a CVD process, or transferring a design across different reactors.[72] The relative importance of pairs of physical phenomena, such as conduction and convection, can be described by various dimensionless numbers.[73–75] In a simplistic view, the mass flow regime in a lab-scale CVD reactor should generally be continuous (low *Knudsen number*, $K_n < 10$, achieved under low to medium vacuum), laminar (low *Reynolds number*, $R_e < 100$, determined by typically 'low' flow rates of the precursors), and diffusion-dominated (low *mass Peclet number*, $P_e < 10$, given by typically 'low' flow rates of the precursors). These regimes should be adjusted to attain different desired outcomes, such as growth rate vs. uniformity. Similarly important is the estimation of the heat transfer (e.g., *Prandtl number*, *Pr*, and *Rayleigh number*, *Ra*) and the surface reaction mechanisms (*Damkohler numbers*, *Da* and Da_{II}). When scaling-up or transferring a CVD process, the dimensionless numbers across the reactors should remain the same in order to achieve reproducibility of results. Modelling methods, such as computational fluid mechanics (CFD), are valuable means to get additional

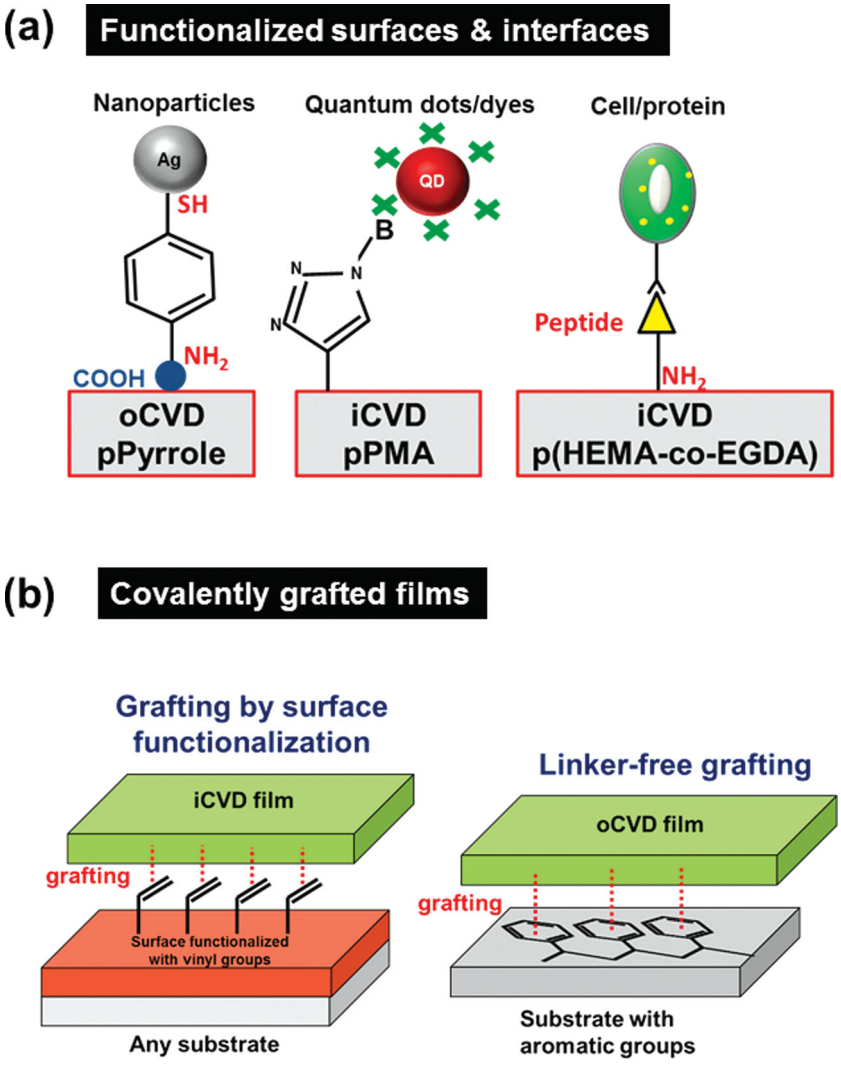

Figure 6. (a) 4-aminothiophenol linker molecules can be used to covalently attach silver nanoparticles to the –COOH groups on surface of oCVD poly-pyrrole film.[55] Azido-biotin (B) linker is used to attach streptavidin conjugated quantum dots to iCVD poly-propargylmethacrylate (pPMA) film.[56] iCVD copolymerized p(HEMA-EGDA) films functionalized with a peptide sequence promotes cell culturing.[57] (b) Surface functionalization of substrates with vinyl groups covalently grafts iCVD grown films to these substrate.[56,58,59] In linker-free grafting, substrates with aromatic groups can be directly grafted to oCVD films.[40,60]

customized insight into the reactor flow patterns and temperature gradients.[76]

The scale-up of polymer CVD process aims to accommodate larger-area stationary substrates, or flexible substrates delivered in form of a roll-to-roll mode (R2R). Both types of processes have been successfully demonstrated. Large-scale batch reactor (Figure 7b) has been employed by GVD Corporation for iCVD of fluorocarbon and silicon polymers,[77] while Gupta et al.[71] have demonstrated R2R iCVD deposition of poly(glycidyl methacrylate) films on flexible substrates. The latter case illustrates that the polymer CVD processes are compatible with already established technologies, and as such, can even be further co-integrated with other non-CVD deposition methods (e.g., spraying, printing, or vacuum thermal evaporation). A proposed scenario can be seen in Figure 7c, where a medium vacuum oCVD process for deposition of transparent conductive PEDOT anode is combined with high-vacuum physical vapor deposition of molecular semiconductors and metallic cathode into a single hybrid R2R line for large-scale production of organic solar cells.

The transfer of various CVD techniques to industrial scale has been steadily growing.[78] CVD polymerization is not only attractive to the scientific community, but also offers several practical advantages when considering scale-up:

- solvent-free processing with relatively low energy input (low temperature, low-medium vacuum);
- one-step polymerization/deposition process eliminating a need for design and synthesis of inks;
- new technology or use of different/additive precursors not required for deposition at different scales;
- non-contact deposition method with well-controlled film thickness and uniformity at large-scale;
- predictably sufficient deposition speeds[71] and established 'know-how' from inorganic CVD.[78]

Design of a reactor for commercial coatings should be governed by the target application and compatibility of the process with the other manufacturing steps. Special consideration should be given to the value of the manufactured products, capital costs, cost of the precursors, operating costs, and possibly the cost of recovering or safely disposing of unconverted reactants.[79]

Finally, the market selection is an important parameter for successful commercialization of any new technology. The range of applications of polymer CVD is in part predetermined by the excellent film properties and deposition capabilities. The current market has already allowed for the creation of a number of companies offering 'conformal nano-coatings' for industries ranging from transportation to medicine.[80–83] Online videos of CVD-coated smartphones functioning even after immersing in water are one such example.[84]

2. CVD Polymer Interfaces for Energy Harnessing and Storage

2.1. Photovoltaic Energy Harnessing

Development of renewable energy sources is critical for replacement of the fossil-fuel economy and delocalization of energy generation. Photovoltaics (PV) comprising of solar

Table 1. Characteristics of iCVD and oCVD polymerization for surface and interface engineering in sustainability related applications.

Property	iCVD and oCVD polymerization	Applications for sustainability
Solvent-free	· High purity films vapor phase films are free from residual solvent contamination	· Photovoltaics[63–65]
	· Reduced materials wastage	· Self-cleaning textiles[51]
	· Suitable for delicate/ natural substrates (e.g., paper)	· Pharmaceuticals, crop protection[10–12]
	· Stacked films, graded and co-polymerized films from immiscible monomers possible	· Biodiesel production[13]
Multi-scale thickness control	· Precisely control film thickness from 10 s of nm to 10 s of μm	· Ultrathin coatings for high permeation water desalination membranes[66]
	· Films can be simultaneously patterned	· Free-standing membranes for water desalination, fuel cells[67]
		· Bio, food, air sensors[14–16]
Thickness uniformity/ conformality	· Ultra-uniform and conformal films possible on non-planar geometries of various aspect ratio	· Photovoltaics,[63–65]
	· Fast film growth rate (>100 nm/min) in iCVD	· DSSC solid-state electrolyte[68]
	· Deposition rate in oCVD limited by oxidant delivery	· Lithium ion battery electrodes[69]
		· Supercapacitors[70]
100% functionality retention	· Low temperatures needed to initiate polymerization fully retain monomer functionality	· Bio, food, air sensors[14–16]
	· Tunable film properties through surface functional groups	· Antifouling surfaces for water desalination[66]
		· Hydrophobic water shedding surfaces for air conditioning, power generation[39]
Energy, cost, scale-up, environment	· Mild, low-power, medium vacuum, scalable processes	· Roll-to-roll printing of photovoltaics[71]
	· Environmentally benign (less waste)	· Low cost drug delivery[9]
	· Fast, single-step processing	· Low power distributed sensing of air quality[14–16]

cell devices which convert solar energy directly into electricity are a key component of this plan. In fact, silicon-based solar cells have already achieved grid parity in many regions of the world.[85] However, emerging solar cell technologies based on organic/polymeric and hybrid materials show significantly higher promise, by reaching commercially attractive efficiencies of 12–15%, while keeping the production costs low.[86,87] The main advantage of organic photovoltaics (OPV) is its integration capabilities – the active films can be deposited on non-conventional substrates, allowing widespread application of the technology onto the objects of everyday life.

Conventional organic solar cell consists of an active layer of organic semiconductors sandwiched between two electrodes, one of which needs to be transparent in order to allow the sunlight to reach the photoactive materials. The transparent electrode is one of the limiting elements of the device.[88] It has relied predominantly on the use of expensive and brittle oxides (e.g., indium thin oxide, ITO), resulting in compromised functionality on flexible substrates. In recent years, poly(3,4-ethylenedioxythiophene) (PEDOT) has emerged as an alternative due to its excellent conductivity, transparency, and mechanical properties.[89] PEDOT has been widely adopted by the OPV community not only as a transparent electrode, but also as an interface layer for enhanced charge transport and injection. High-conductivity PEDOT films have been fabricated by multiple methods – standard solution processing ($\sigma \approx 3300$ Scm^{-1}),[90] vapor-phase polymerization ($\sigma \approx 3400$ Scm^{-1}),[91] and oxidative chemical vapor deposition ($\sigma \approx 2800$ Scm^{-1}, latest result from our lab submitted for publication). In particular, solvent-free oCVD PEDOT has been successfully applied in multiple advanced OPV architectures, demonstrating versatility of the deposition technique, its substrate independence and conformality.[63–65]

Conductivity of oCVD PEDOT can be largely improved through elevated substrate temperature and post-processing treatment with weak acids.[30,44] The former leads to a longer conjugation length and enhanced packing of the polymer, and the latter results in better dopant exchange and a higher degree of doping. Howden et al.[44] illustrated the latter by rinsing PEDOT films with 1M H_2SO_4 and 1M HBr, removing excessive $FeCl_3$ oxidant and achieving improved film stability and over 100% increase in film conductivity. Similar strategies have been used also for PEDOT:PSS.[92] However, any post-deposition treatments limit the choice of device architecture and put more restrains on scale-up. Elimination of rinsing steps by ensuring that efficient doping takes place during the deposition process would therefore be preferred. In fact, Hitesh et al. demonstrated a completely dry oCVD process to deposit PEDOT films, using bromine as oxidant. The lower volatility and oxidation potential of bromine compared to chlorine made the resultant PEDOT films exhibit enhanced stability, retaining high electrical conductivity during accelerated aging experiments in air. Stability is critical for application of oCVD grown PEDOT films in OPV devices.[93] Improvements in conductivity would also benefit from more detailed studies of the fundamental mechanisms of conduction in oCVD PEDOT, as well as from better understanding of the structure-property relationships. These topics are currently under investigation.

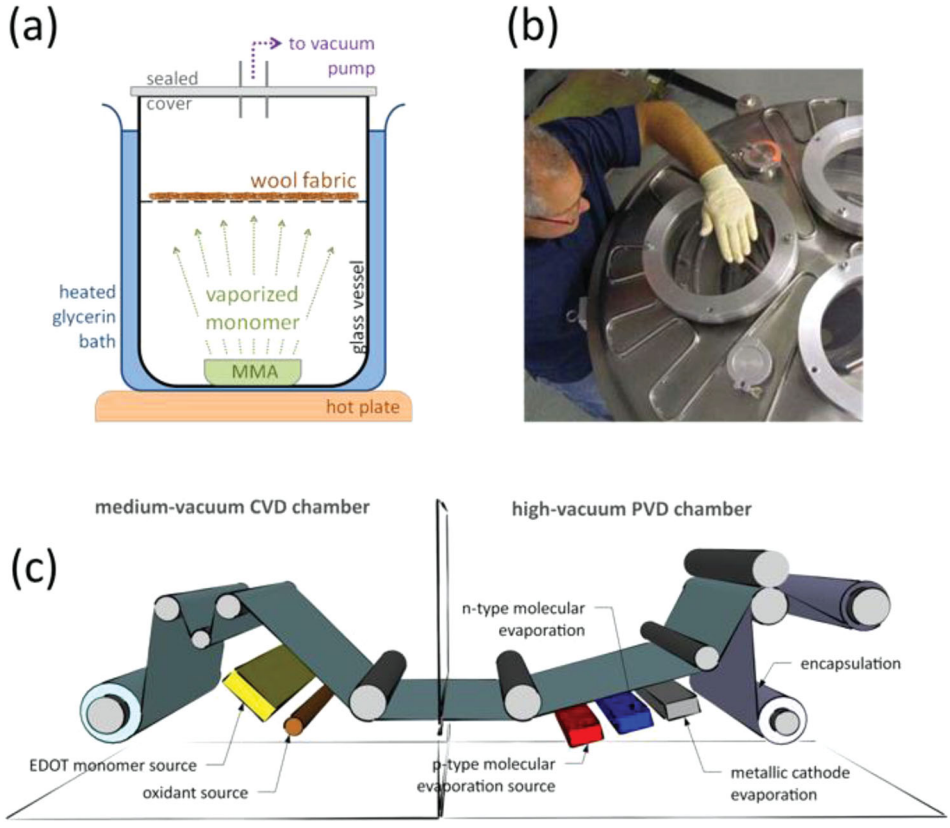

Figure 7. (a) Example of a simple CVD reactor for coating of wool fibers with UV-protecting PMMA.[49] (b) Large-scale batch reactor for commercially coating objects with fluorocarbon and silicon polymers (image is courtesy of GVD Corporation, Cambridge, Massachusetts, USA). (c) Sketch of a basic roll-to-roll line for production of organic solar cells using hybrid double-chamber system for oCVD deposition of PEDOT transparent anode (left) and vacuum thermal evaporation of molecular semiconductors together with metallic cathode (right). (a) Reproduced with permission.[49] Copyright 2013, American Chemical Society.

Conformal PEDOT produced by oCVD plays multiple key roles in wider application of OPVs – it can be deposited and hence serve as an electrode on almost any substrate; it binds covalently to many surfaces lowering the chance of device delamination; it can act as a planarizing interface layer for rough substrates, decreasing a chance of device shunting when the subsequent thin films are deposited by standard thermal evaporation or solution techniques.[63] Organic solar cells have tremendous integration advantages and their future is unlikely to stay on glass. Deposition of OPV on surfaces, such as paper or textiles, is therefore an essential step in realizing the full potential of the technology. Initial studies on paper solar cells using oCVD PEDOT both as a bottom[63] and a top[65] electrode have demonstrated that efficiencies comparable to plastic- and glass-based devices can be achieved. **Figure 8**a displays top-illuminated OPV devices[65] deposited on different substrates (on left), with the respective *J*–*V* curves plotted (on right). The optoelectronic characteristics show that the solar cell on high-quality stamp paper (thick dashed line, η_{stamp} = 2.0%) reaches similar power conversion efficiency to its counterpart on plastic (thin dashed line, $\eta_{plastic}$ = 2.2%), and also compares well with the reference sample on glass (solid line, η_{glass} = 2.8%). However, the other curves indicate that the surface roughness of the substrate plays an important role in the device performance, compromising the efficiency for devices on photo paper (solid line, η_{glass} = 1.5%) and magazine paper devices (solid line, η_{glass} = 0.4%) through increased current shunting. Although textile-based devices have not yet been fabricated, Bashir et al. have successfully produced conductive viscose and polyester yarn fibers using VPP PEDOT.[94–96] Much work still needs to be done to deposit a multilayer device on textiles, especially when aiming for its sustained functionality under mechanical stress.

Enhancement of power conversion efficiency is another critical area for OPV research. There are two main approaches working in synergy here, namely the molecular design of organic semiconductors, and the architectural design of the OPV device.[100] Synthetic chemistry targets appropriate position of the energy levels and character of the film morphology, while the device architecture helps to overcome fundamental efficiency barriers such as the Shockley–Queisser limit. Nanophotonics stands out as an attractive solution for efficient light management in solar cells.[101] Light-trapping and light-directing features can be fabricated at one of the electrode interfaces, enhancing photon absorption and leading to significant efficiency improvements (schematically depicted in Figure 8b). Light management techniques require features with intricate nanoscale morphology, and thus necessitate a conformal coating of the polymer layer, when such textured surfaces are

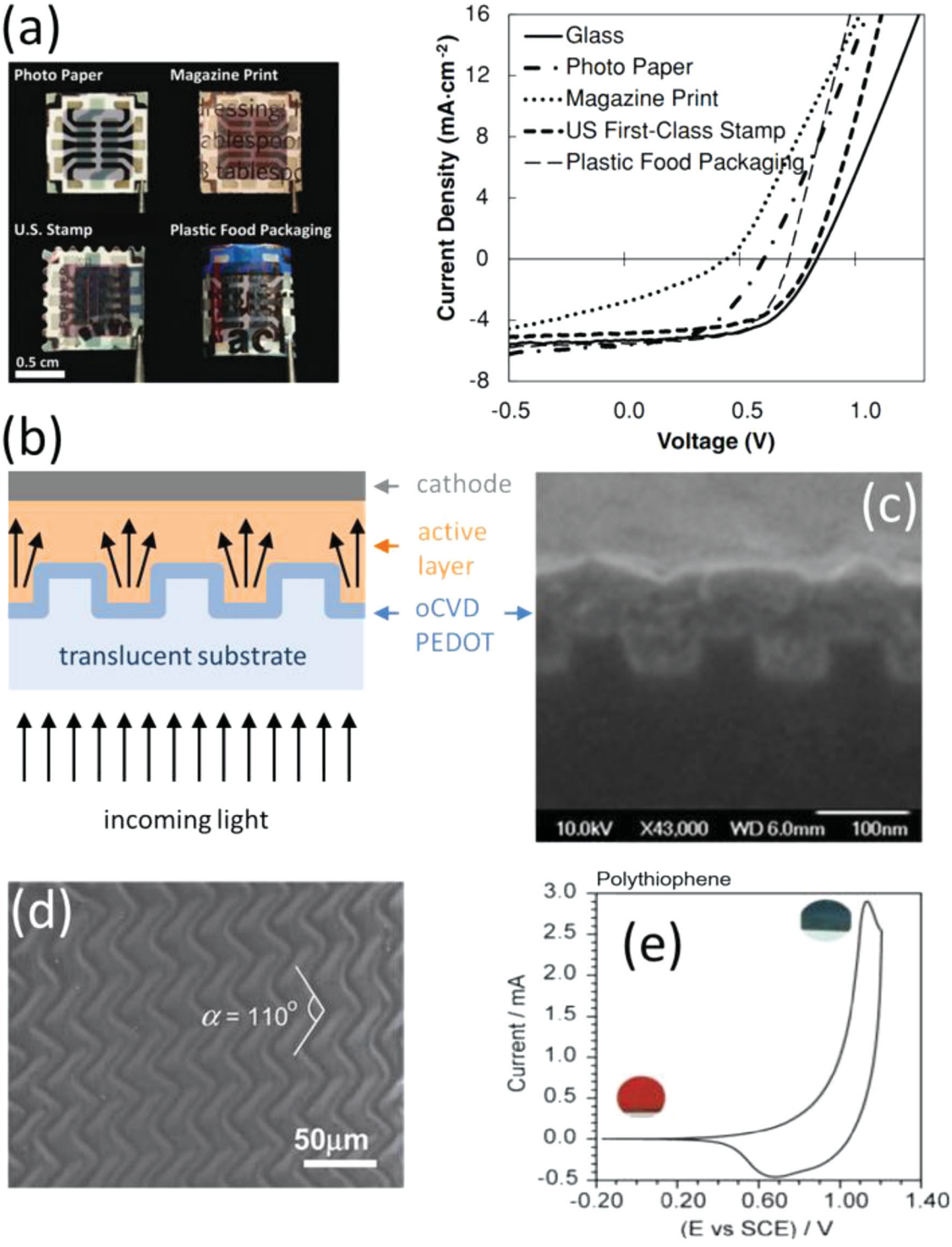

Figure 8. (a) Top-illuminated organic solar cells deposited on different opaque substrates (left) and their respective *J-V* characteristics (right).[65] (b) Schematics of light-trapping OPV device with a textured substrate conformally coated by oCVD PEDOT and (c) SEM of such photonic structure with PEDOT on top.[97] (d) Controlled wrinkling of a iCVD grown pHEMA film by stretching of the PDMS substrate.[98] e) Electrochromic behavior of unsubsituted polythiophene films deposited by oCVD.[99] (a) Reproduced with permission.[65] Copyright 2012, Wiley. (c) Reproduced with permission.[97] Copyright 2013, Elsevier. (d) Reproduced with permission.[98] Copyright 2012, Wiley. e) Reproduced with permission.[99] Copyright 2011, American Chemical Society.

used as a device substrate. As shown in Figure 8c, Howden et al.[97] demonstrated that photonic features as small as 10s of nm in size can be conformally coated by PEDOT deposited via oCVD. The PEDOT electrode retains its conductivity, while the textured substrate geometry results in an increased absorbance of the semiconductor films deposited on the top.

There are also other strategies for producing devices with light-trapping topography, two of which are depicted in Figure 8d and e. The left image shows controlled wrinkling of a polymer film through directional stretching.[98] To avoid delamination, iCVD polymer films can also be covalently grafted to the substrate, as previously discussed in section 1.2.2. Similarly, oCVD PEDOT bonds covalently to many plastic substrates, allowing stretchability of films deposited on textured plastic surfaces.[60] Enhancement of light absorption and photovoltaic efficiency through such texturing and wrinkling techniques has been shown previously.[102] Another approach could be based on a conductive scaffold with features at the scale of the incoming light wavelengths, as shown earlier in Figure 3d. The scaffold forms after the dissolution of templating polystyrene beads conformally coated with conductive PEDOT.[40] These are just some of the examples that illustrate the great promise of oCVD in fabricating advanced photonic architectures using low-cost methods with the potential for large scale deployment.

The molecular design of organic semiconductors has been a significant contributor to the recent progress of the OPV field.[103] However, the photoactive molecules are designed almost exclusively for wet methods and hence continue to encounter the same processing issues. While such polymers can be modelled and designed to have excellent optoelectronic properties, their poor solubility and film morphology often hinder further application. Synthesis of semiconducting polymers for OPV has also been investigated by oCVD[32] (using the same $FeCl_3$ oxidative polymerization methods used for PEDOT films). The advantage of this method is the absence of solvents, which removes the restrictions on polymer solubility. The aforementioned benefits of oCVD along with this ease of processing can enable the complex OPV device architectures required to reach higher efficiencies.

As a proof of concept, oCVD films of semiconducting polymers like polythiophene (PT) have been successfully synthesized, and applied as active layers in OPV devices.[104] The thickness-optimized planar heterojunctions based on PT/C_{60} matched the performance of the PT-based devices fabricated by other techniques. It is worth mentioning here that unsubstituted PT is difficult to process by solution-based techniques due to the insolubility of the monomer. Nejati et al. further showed that oCVD grown PT films displayed electrochromic behavior.[99] As indicated by cyclic voltammetry (CV) curves in Figure 8e, while these films are orange-red in the initial doped state at 1.1 V, they turn blue in the de-doped state at 0.6 V. Such films find use in energy-saving electrochromic windows, which can intelligently control the amount of light passing through a window. In addition to PT, semiconducting homopolymers with a wide range of bandgaps (1.1 – 2.0 eV) have also been processed, such as polyselenophene (PSe),[105] and polyisothianaphthene (PITN)[106] (**Figure 9**a). Borrelli et al.[106] demonstrated efficient bandgap engineering of PITN simply by changing the substrate temperature during the deposition/polymerization. As shown in Figure 9b, a change in substrate temperature by an interval of 60 °C results in a shift of the absorption maximum of PITN by more than 100 nm. Such tuning of optoelectronic properties could be further advanced by co-polymerization, while ensuring the high degree of regioregularity necessary for molecular order.

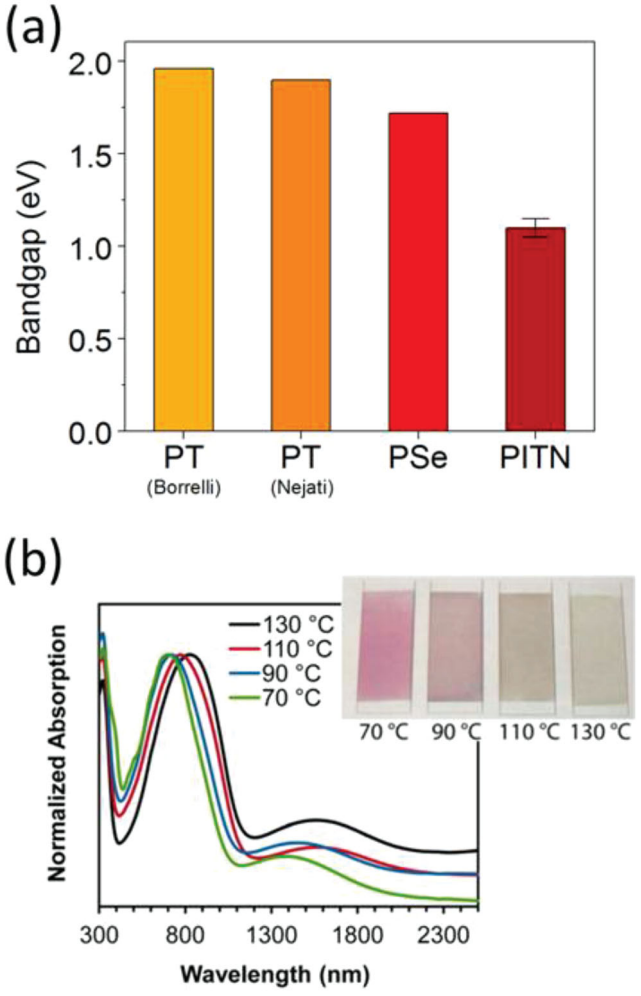

Figure 9. (a) Bandgap energies for different polymers obtained by oCVD.[99,104–106] The deviation bar for PITN shows a range of bandgaps achieved using different substrate temperatures. (b) Shift of PITN peak UV-Vis absorption due to different substrate temperatures.[106] Inset: As-deposited PITN films on glass slides. (b) Reproduced with permission.[106] Copyright 2013, American Chemical Society.

The application of polymer CVD in photovoltaics is not only in the area of electronically active layers. There is also considerable potential for the use of dielectric polymer films produced by iCVD as passive components. For example, Rong et al. performed passivation of silicon using iCVD-grafted dielectric films of poly(ethylene glycol diacrylate) (pEGDA).[61] This treatment is low-temperature and inexpensive, yet it achieves a decrease in the surface recombination of minority carriers (≤10 cm s^{-1}) comparable to what can be obtained from current commercial technologies. These films (grafted by the iCVD equivalent of linker-free grafting in Figure 6b) were also demonstrated as anti-reflection coating (ARC) layers in silicon solar cells.

The films deposited by the iCVD method are pinhole-free, a feature which has largely been explored for the encapsulation of air-sensitive materials. Some of the most successful approaches have relied on iCVD deposition of organic or organosilicon coatings, often accompanied by interlayers of Si-based inorganics processed by PECVD or HWCVD.[107–114] Multilayer

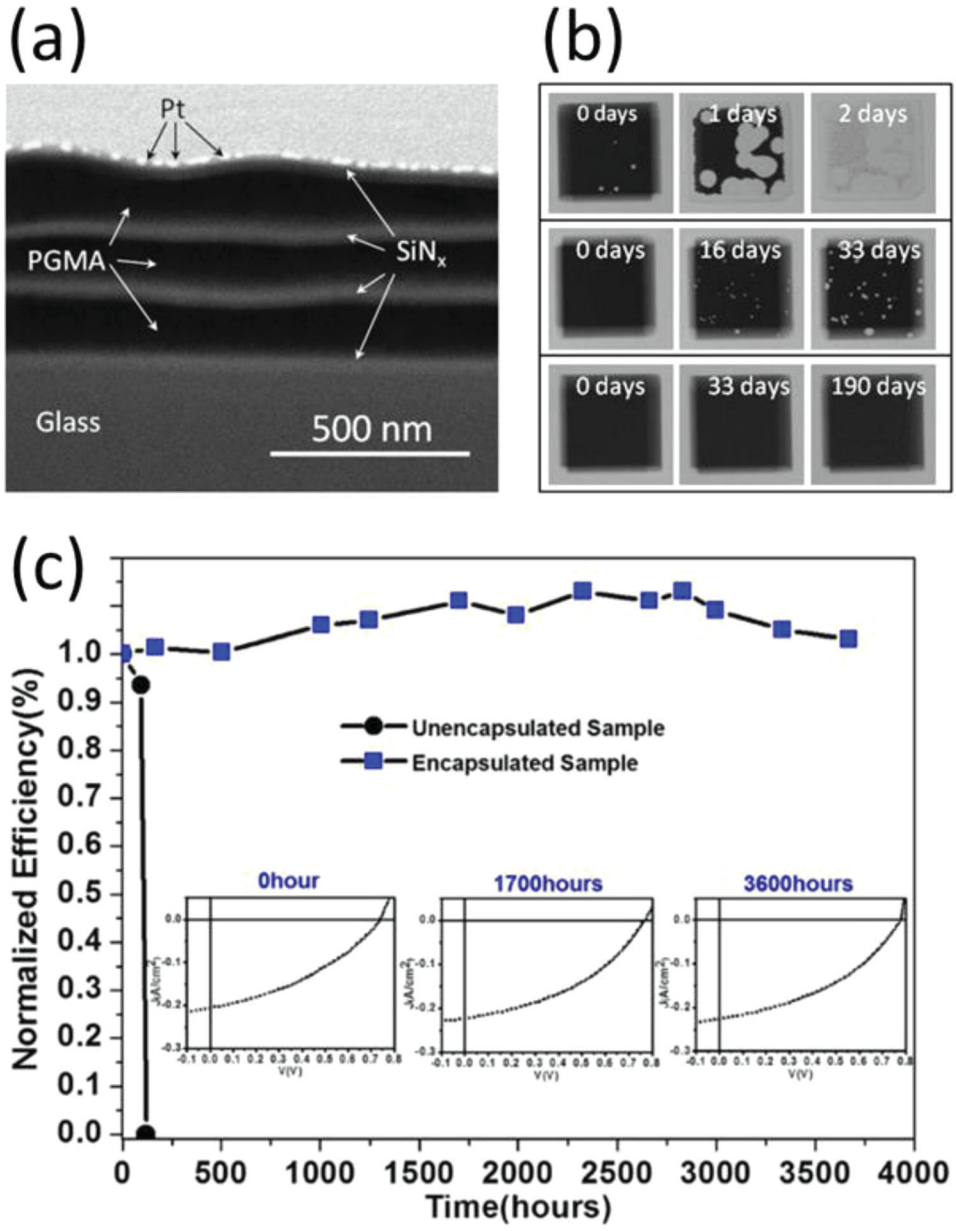

Figure 10. a) Multilayer encapsulation barrier based on alternating layers of SiN_x and PGMA.[108] b) Oxygen-sensitive Ca test of low-temperature deposited SiN_x barrier (top row), high-temperature deposited SiN_x barrier (middle row), and SiN_x-PGMA-SiN_x multilayer barrier.[108] c) Encapsulation test of the OPV device stability with depicted *J–V* characteristics of the device after 0 h, 1700 h, and 3600 h.[115] (a) and (b) Reproduced with permission.[108] Copyright 2013, Elsevier. (c) Reproduced with permission.[115] Copyright 2013, IOP publishing.

stacks of organic/inorganic layers, as depicted in **Figure 10**a, lead to extremely low permeation rates of water vapor and oxygen – their performance increasing with the number of layers within the stack.[108] Figure 10b shows an oxygen-sensitive Ca test comparing the encapsulation properties of a single layer of low-temperature deposited SiN_x (top row), a state-of-the-art high-temperature deposited SiN_x (middle row), and a double-layer of SiN_x sandwiching a layer of poly(glycidyl methacrylate) (PGMA) (bottom row). The difference in barrier properties is significant. The three-layer SiN_x/PGMA structure, shown in Figure 10a, has a water vapor transmission rate (WVTR) of only 5×10^{-6} g/m^2/day at 60 °C and a relative humidity of 90%, which makes it a suitable candidate for encapsulation of OPV and OLED technologies. Recently, Li et al. presented a new single-layer barrier using hybrid organosilicon hexamethyldisiloxane (HMDSO) deposited by PECVD.[115] The low WVTR of 3.6×10^{-6} g/m^2/day was demonstrated on encapsulation of OPV devices containing air-sensitive active layers. As seen in Figure 10c, the device lifetime was extended from 120 h for the unencapsulated sample, to over 3600 h for the HMDSO-encapsulated sample. Finally, Barr et al. demonstrated that iCVD encapsulation of paper PV devices containing oCVD PEDOT electrodes not only extends lifetime, but adds water-proofing functionalities allowing the devices to operate while submerged under water.[63]

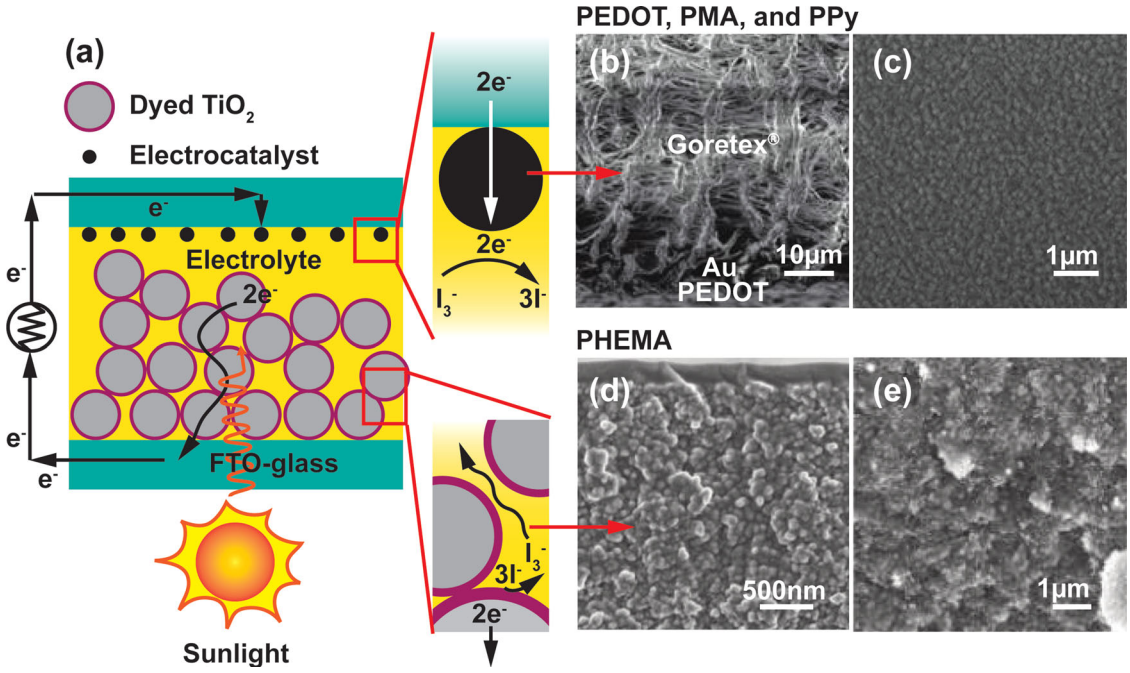

Figure 11. (a) Electron flow and redox reactions that occur in the interfaces of dye sensitized solar cells, in which VPP could be applied to replace electrocatalyst and liquid electrolyte. Scanning electron microscopic images of (b) PEDOT deposited by VPP/Au/PMA/Goretex cathode.[117,119] (c) Polypyrrole (PPy) synthesized by VPP.[120] Mesoporous TiO_2 of thickness (d) 3 μm, (e) 12 μm completely filled with pHEMA as a hole conductor.[68] (b, d-e) Reproduced with permission.[119,120] Copyright 2010, 2011, American Chemical Society. (c) Reproduced with permission.[68] Copyright 2011, Royal Society of Chemistry.

2.2. Electrochemical Energy Conversion

2.2.1. Dye-Sensitized Solar Cells (DSSCs)

Dye-sensitized solar cells (DSSCs), which rely on photo-electrochemical processes to generate electricity, have garnered tremendous scientific interest since they were invented by Grätzel in 1991. DSSCs recently achieved high conversion efficiency, ~15%, as desired for commercialization.[116,117] In the original structure, a DSSC consists of a photoanode comprising of mesoporous TiO_2 sensitized with dye molecules, a cathode with Pt serving as an electrocatalyst, and an iodine-based liquid electrolyte between the electrodes as shown in **Figure 11**a. VPP requires pre-application of oxidant before introducing the EDOT vapor. Sirimanne et al. synthesized PEDOT:para-tolunesulfanate (PTS) by introducing EDOT vapor to Fe^{III}-para-toulensulfonate coated glass at 70 °C for 1 h, producing the lowest sheet resistance (4 Ω/□) for ~20 μm thick film.[118] The PEDOT:PTS on plain glass was found to have both conductive and catalytic properties. For DSSCs, an optimal PEDOT:PTS film thickness of ~10.2 μm achieved an overall DSSC conversion efficiency of 5.25%, which is remarkably comparable to the 5.58% obtained with Pt.

In Figure 11b, Mozer et al. deposited a PEDOT catalyst layer using VPP on a PTFE (polytetrafluoroethylene, Goretex) membrane.[119] Prior to the deposition of PEDOT, they deposited poly(maleic anhydride), pMA on one side of the membrane with low-power plasma polymerization to promote good adhesion between the PTFE layer and Au electrode, and then sputtered Au to reduce the sheet resistance. VPP using Fe^{III}PTS as the pre-applied oxidant enables the PEDOT film to form on one side of the fluoropolymer membrane. This compressible and stretchable cathode is potentially beneficial to solid-state DSSCs because its 60% compressibility and 80% porosity can make good electrical contact with uneven mesoporous TiO_2 film on the photoanode. Yet another example for polymer based DSSC electrocatalysts is the VPP based synthesis of polypyrrole (PPy) at room temperature on fluorine doped tin oxide (FTO), by Xia et al. (Figure 11c). When compared to PPy synthesized by electropolymerization (EP),[120] the VPP-PPy displayed a distinct I^-/I_3^- redox reaction in cyclic voltammetry (CV) measurement, similar to that of Pt. This is because the VPP utilized larger, less mobile doping anions, toluene sulfonate, TsO^-, as compared to the perchlorate anions, ClO_4^- used in EP. The performance of VPP-PPy in DSSCs was dependent on the concentration of oxidant during VPP, which was ascribed to the coverage of PPy on FTO-glass and the interface between PPy and FTO-glass.

Less volatile solid or quasi-solid-state electrolytes have also been proposed to substitute volatile liquid electrolytes (e.g., iodine in acetonitrile) used in DSSCs. Their performance as hole conductors, however, has typically been inferior to liquid electrolytes because it is difficult to completely fill solid electrolytes into the pores of the > 10 μm thick mesoporous TiO_2 film in the photoanode. Interestingly, the conformality of the iCVD process enabled Nejati et al. to achieve complete pore filling of ~12 μm thick mesoporous TiO_2 with poly(2-hydroxyethyl methacrylate) (pHEMA) films.[68] Based on reaction and transport kinetics, they systematically investigated the process parameters in iCVD that improve pore filling. The P_M/P_{sat} ratio discussed in section 1.2.2 was found to be the most important

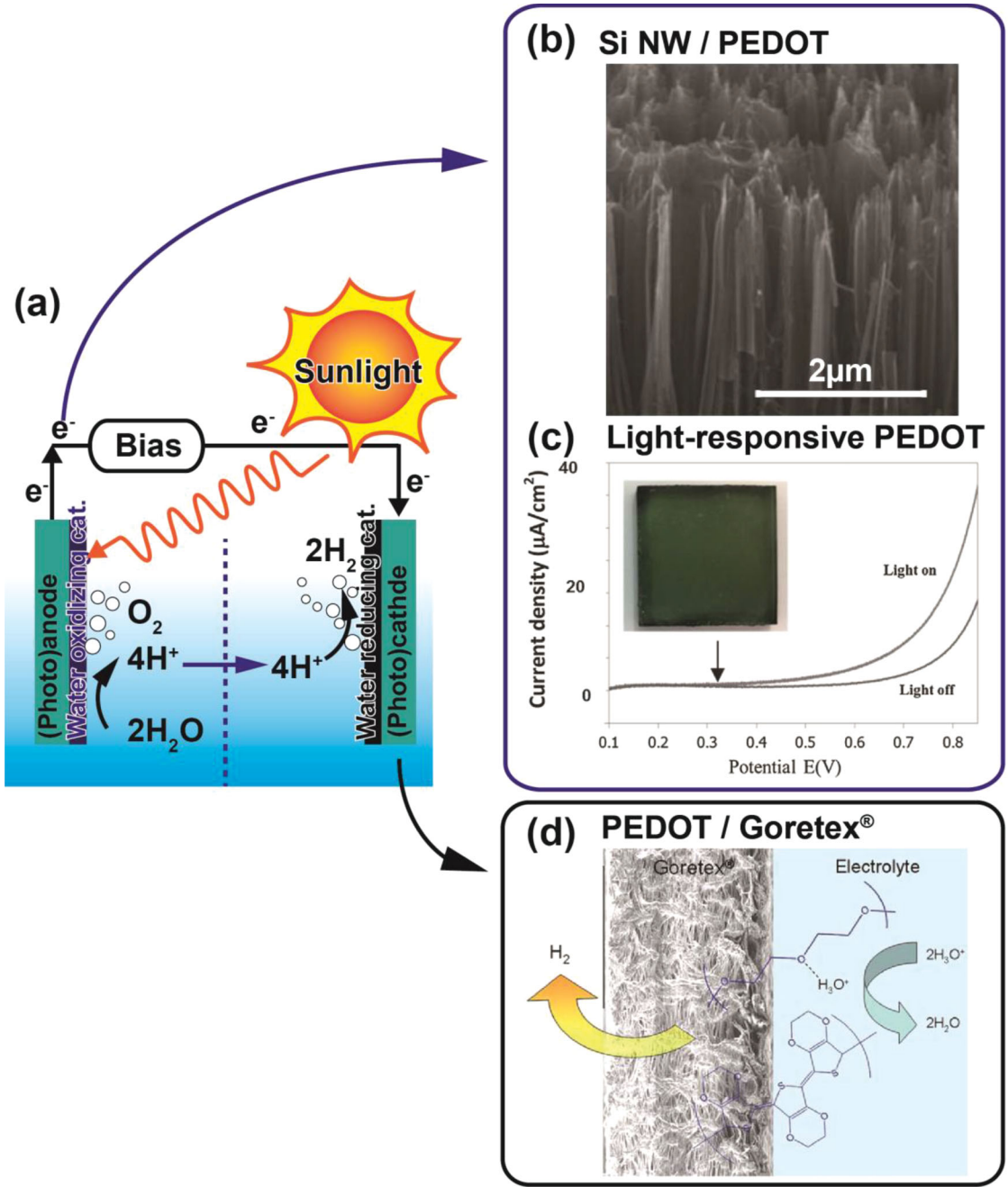

Figure 12. (a) Schematic of the working principle of water splitting (b) PEDOT coated Si nanowires (Si NW/PEDOT)[121] (c) light-responsive PEDOT on FTO-glass for water oxidation.[122] (d) PEDOT/Goretex electrodes for water reduction.[123] In (b–d) PEDOT was synthesized by VPP. (b-d) Reproduced with permission.[122,123] Copyright 2011, 2013, Royal Society of Chemistry.

iCVD process parameter that controls pore filling. Figures 11d and e represent the complete pore filling of mesoporous TiO_2 (4 and 12 μm thick, respectively) under the optimal conditions they determined.[68]

2.2.2. Catalytic Water Splitting

Hydrogen production from water using solar energy or electricity is an emerging technology for generating alternative fuel for transportation and for large-scale industrial use. **Figure 12**a is a schematic that describes how water splitting occurs. Li et al. demonstrated PEDOT coated Si nanowires (Si NW/PEDOT) using VPP for water oxidation as shown in Figure 12b.[121] The PEDOT acts both as a catalyst and as a barrier against photocorrosion. The PEDOT conformally covered the Si NWs keeping the interfaces between Si NW and PEDOT perfectly intact. Because of the good adherence and pin-hole free coverage of the PEDOT films onto the NW surface, the PEDOT film effectively isolates the Si NW from aqueous electrolytes, improving

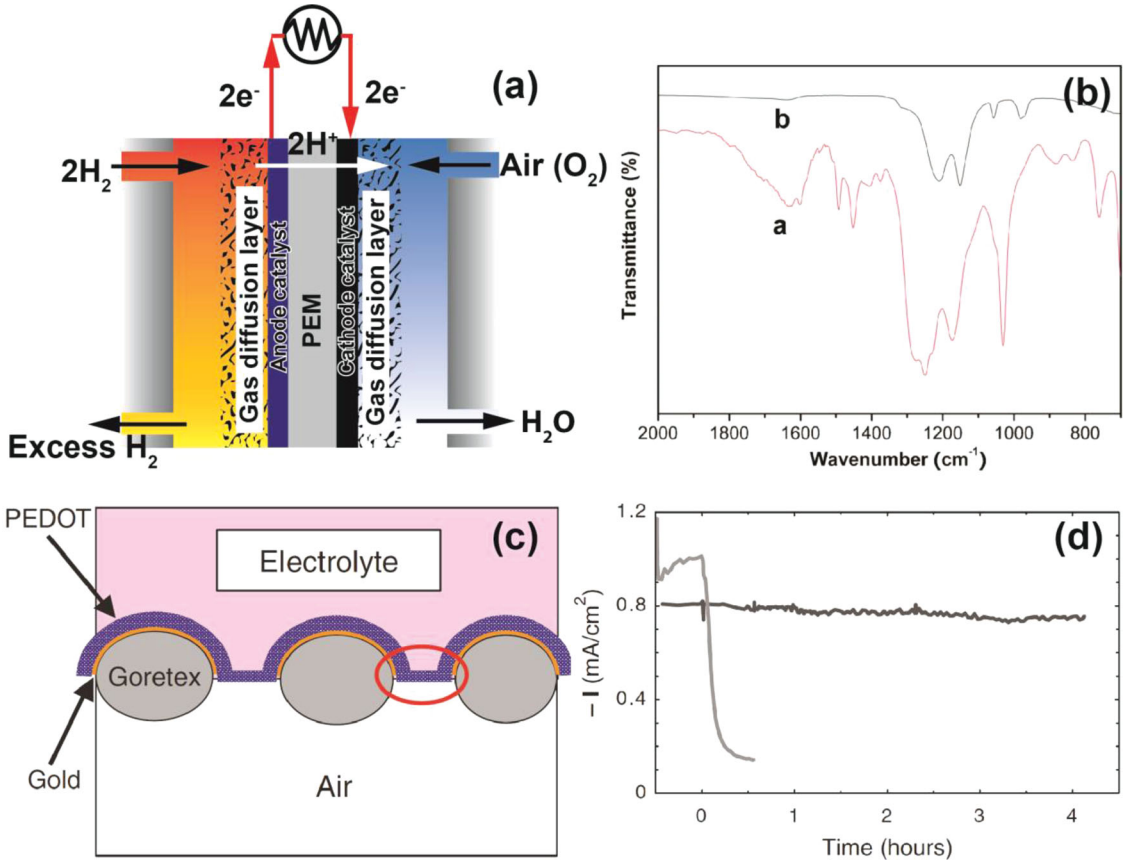

Figure 13. (a) PEM fuel cells (b) FTIR spectra of plasma PEM (black line) and Nafion® 117 (red line)[137] (c) Schematic diagram of the PEDOT/Goretex air electrode[139] (d) Decaying currents versus time of PEDOT/Goretex (black line) and Pt-catalyzed electrode (gray line) under air contaminated by 10% CO.[139] (b) Reproduced with permission.[137] Copyright 2012, Royal Society of Chemistry. (c-d) Reproduced with permission.[139] Copyright 2008, AAAS.

the electron-hole separation at the interface of Si NW and PEDOT.

Recently, Chen et al. showed the potential of VPP to deposit PEDOT films on FTO-glass and plastic substrates, which serve as a photocatalyst layer for splitting seawater.[122] They incorporated high levels of sulphonated manganese porphyrin dimers into PEDOT resulting in a light-responsive PEDOT film with the maximum absorbance at wavelength λ = 443 nm. It is interesting that VPP PEDOT demonstrated photocatalytic effect while EP PEDOT did not. This is clear evidence that the phorphyrin dimers are fully incorporated into the PEDOT backbone by VPP. This key feature was also confirmed by the excitonic couplings of porphyrin dimers in UV-vis absorbance.

Winther-Jensen et al. deposited PEDOT on Goretex membrane with VPP to reduce water and form hydrogen, as depicted in Figure 12d.[123,124] Interestingly, they found that when non-conducting polymers like polyethylene glycol (PEG) were integrated with PEDOT, the resulting PEDOT-PEG showed superior electrocatalytic properties (electrochemical over-potentials and current density) compared to pure PEDOT. This is because PEG helps transport protons or H_3O^+ to the catalytic sites on PEDOT. The strategy is also applicable to other conducting polymers like PPy, mentioned in the DSSC section.[120]

2.2.3. Fuel Cells

Figure 13a describes proton exchange membrane (PEM) fuel cells in which oxygen in air and hydrogen as a fuel arrive at respective electrodes, and react to produce electricity and water as a byproduct. Two electrodes sandwich the PEM, which allows only protons (H^+) to move to the cathode. While plasma-enhanced CVD (PECVD) has been extensively explored for synthesizing PEMs, iCVD was recently used to grow PEM comparable to commercial Nafion® for the first time.[125–137] The PEM should be inherently robust, have high ionic conductivity, and also be impermeable to fuels under the acidic and high temperature operating conditions of fuel cells. Highly cross-linked PECVD polymers offers stability and low fuel permeability, but provides only partial retention of the functional groups responsible for the ionic conductivity. Lower power, pulsed plasma, and modified plasma discharges have been explored as means to retain more sulfonic acid (-SO_3H), phosphoric acid (-PO_3H), and carboxylic acid (-COOH) groups in the polymer backbone.[130,137,138] As indicated by the Fourier transform infrared (FTIR) spectra in Figure 13b, the characteristic peaks of PECVD PEM are similar to, but not exactly identical to, those of Nafion® 117. In particular, PECVD PEM shows the clear absorbance of -SO_3H group around 1030 cm^{-1}.[137] While

the plasma in PECVD reduces functional group retention, the mild nature of the iCVD process was recently used to synthesize hybrid fluoro-carboxylated copolymers for PEM, which completely retained their acid and hydrophobic functionalities. This novel PEM achieved high ionic conductivity of 70 mS/cm comparable with Nafion® and exhibited good stability under water.[136] This example demonstrates that the iCVD process has potential for synthesizing high performance fuel cell PEM with 100% functionality retention.

Polymer films have also been explored as the electrocatalyst in fuel cells. Winther-Jensen et al. found that PEDOT with the structure illustrated in Figure 13c exhibits good long-term stability during oxygen reduction, when compared to Pt (Figure 13d).[139] Similarly, Cottis et al. used VPP to grow PEDOT films on a fluoropolymer membrane in the presence of a triblock copolymer to fabricate a metal-free oxygen reduction electrode.[140]

2.3. Electrochemical Energy Storage

With increasing environmental pollution and the rapid depletion of fossil fuels, the need for efficient usage of clean and sustainable energy sources like solar is growing. Nevertheless, daily and seasonal variations in such energy sources, makes simultaneous development of energy storage technologies critical. In many applications (e.g., electronics, power tools, electric vehicles) electrochemical energy storage technologies like electrochemical supercapacitors (ES) and batteries are typically used. Due to their long lifecycle and high power density, supercapacitors (SC), which fill the gap between traditional dielectric capacitors with high power output and batteries with high energy storage, have attracted significant attention.[141,142] ES can also serve as a complementary storage technology to batteries, by providing back-up power supplies in devices.[143] Electrochemical devices are usually composed of an anode and a cathode, an electrolyte and a separator. During discharge, electrochemical reactions takes place at the electrodes, and electrons are generated which move through the external circuit. During charging, an external voltage is applied across the electrodes, for the movement of electrons and reactions at the electrodes. Rechargeable batteries can be classified as lead-acid, zinc-air, nickel-cadmium, sodium-nickel-chloride, sodium-sulfur and Li-ion batteries (LIBs). For portable electronics, LIBs are the most popular due to their many advantages such as light weight, high voltage, low toxicity and long cycling life.

SCs can operate both in the electric double layer mode, based on the separation of charges at the interface between a solid electrode and an electrolyte and the pseudo-capacitive mode, which is a Faradaic process involving electrochemical redox reaction. Materials for such redox reactions include conducting polymers, metal oxides and carbon.[144–146] Polymer films synthesized by various methods have been successfully used in both batteries and SCs. In this section, the advantages of chemical vapor deposition of polymers films for batteries and SC will be discussed. As mentioned in section 1.2.2, the ability to precisely control the thickness and conformality of these polymer films, along with other properties (e.g., conductivity, stability, morphology) can be critical in these devices.

2.3.1. Lithium Ion Batteries

A typical LIB has four main parts, namely the anode, cathode, separator and electrolyte. Li-containing layered, spinel or olivine metal oxides form the cathode and graphite, silicon, TiO_2, etc. typically form the anode. A separator layer (made of plastic) helps prevent short circuiting between the anode and cathode and also facilitates Li ion movement during charging/discharging. For the electrolyte, the most important property is high Li ion conductivity and good electronic insulation. Most commonly used electrolytes are liquid-state (e.g., Li-salts dissolved in organic solvents).[147] During LIB operation, the Li ions shuttle between anode and cathode as the battery is cycled. In spite of offering several advantages, like high energy density and long cycling life, over older battery technologies (e.g., lead-acid, Ni-based batteries), current LIBs are not sufficient for emerging technologies in mobile electronics, electric cars, which demand higher energy and power densities along with longer cycling life. Yet another challenge is the size of the batteries. The future needs are in the direction of small scale and mobile devices for multiple applications (e.g., medical implants, distributed sensing) where the size of the power supply is a critical factor.[148–150]

Currently, large footprint areas are needed to achieve high capacity LIBs. As discussed in the work of Arthur et al. 2D battery designs result in a compromise between energy density and power density due to the limitation in the footprint area.[69] The solution can be designing 3D battery architectures, by taking advantage of the third dimension to increase the electrode material, without increasing areal footprint. The basis for next-generation energy efficient devices, such as electrochemical capacitors and batteries will be 3D nanostructured electrode architectures. This new battery design requires coating a conformal electrolyte (e.g., polymer) layer over the nanostructured 3D electrodes, without pin-holes that can create current shunting paths leading to battery failure. In addition to conformality, the polymer electrolytes must also be doped to obtain good ionic conductivity. The electrolyte layer should also be ultra-thin (e.g., Figure 3a) to promote fast Li ion diffusion kinetics. Transport resistances increase with film thickness, thereby reducing the discharge capacity and rate capability of the LIB, due to the development of concentration polarization at the electrode.[151] This problem can be solved by coating an ultra-thin, conformal, pin-hole free polymer electrolyte layer over the entire 3D electrode, enabling the design of truly 3D LIBs with small areal footprint (**Figure 14**a and b).[152]

Due to its ability to conformally coat complex micro and nanoscale structures (Figure 4), polymer CVD has a huge potential for developing such 3D nanostructured energy storage devices. Indeed, several reports have shown the uniform and conformal coating of ultra-thin polymer films on silicon micro-trenches using the iCVD method.[32] Another example is the coating of carbon nanotubes (CNTs). TEM image of the CNTs coated with a conformal iCVD polymer layer is shown in Figure 14b.[153] CVD enables the deposition of thin polymer films on various substrates with good conformality, an outcome which is difficult to achieve with solution polymerization techniques.[35] Combining the ability of iCVD to produce ultra-thin, conformal polymer electrolyte coatings with novel high capacity

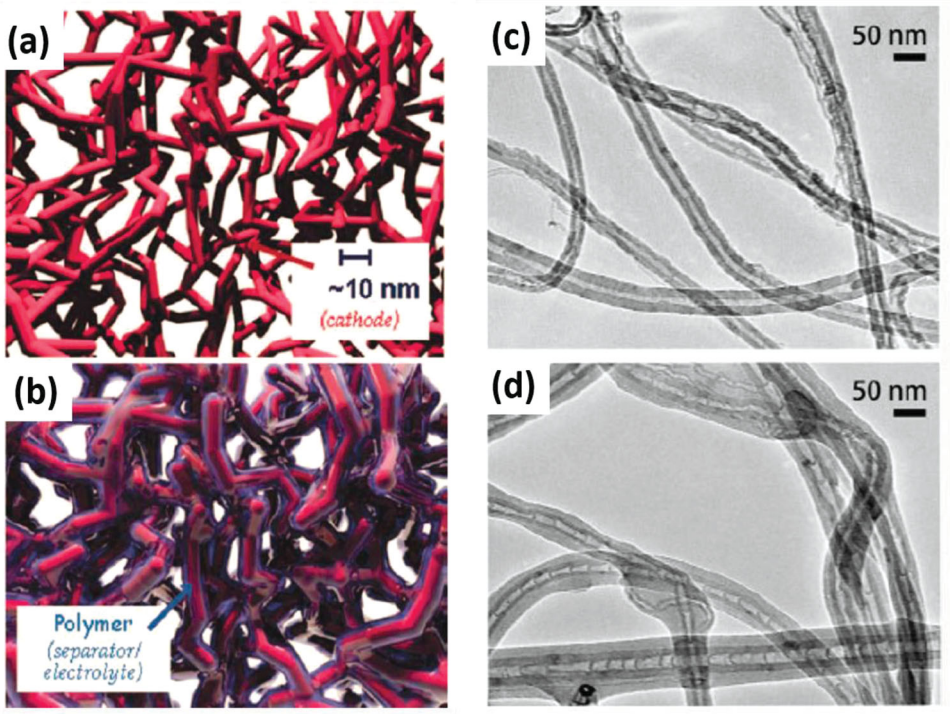

Figure 14. (a) Schematic of a 3D electrode and (b) the conformal coating of a polymer over a high-surface area where the functional components are sized on the order of 10 nm.[152] (c)TEM image of uncoated CNTs, 20–50 nm in diameter, 5–20 μm in length (d) TEM image of conformally coated CNTs 25 nm thick iCVD pGMA.[153] (a,b) Reproduced with permission.[152] Copyright 2014, Royal Society of Chemistry. (c,d) Reproduced with permission.[153] Copyright 2014, John Wiley and Sons.

3D electrodes, thus has the potential for fabricating a new class of lithium ion batteries which exhibit both high energy and high power densities.

2.3.2. Supercapacitors

As mentioned earlier, SCs store energy both with double-layer charging and faradaic processes. In the first process, accumulation of charges (Δq) of opposite signs takes place between solid and ionic solution interfaces, which depends on the potential difference built up across this interface (ΔV). As a result, a capacitance ($C = \Delta q/\Delta V$) is formed known as double layer capacitance in which the charge storage is purely electrostatic and no chemical reactions are involved.[154] In the latter process, redox reactions are involved where the charge (q) is a function of V and derivative of dq/dV is known as faradaic capacitance.[154] This capacitance is 2 or 3 orders of magnitude higher than the double layer systems.[155] When charged, conducting polymers lose electrons causing anions in the solution to move into the polymer to maintain charge neutrality.

There are different methods to synthesize the polymers for supercapacitors, such as electrodeposition,[156,157] solution processing and air brushing.[158] However, all these methods are substrate dependent and thickness control and uniformity is generally difficult.

Carbon based materials and carbon nanotubes (CNTs) are widely used as active electrode materials in SCs due to their high surface area and conductivity.[143,159–162] However in these systems the charge accumulation takes place only at the surface, which limits the specific capacitance. To overcome this problem conducting polymers have been used to coat the CNTs where the entire volume of the polymer is involved in charge storage, hence increasing the capacitance. In the work of Ghaffari et al., PEDOT films were coated on aligned CNTs by oCVD, resulting in a conformal polymer layer all over the CNTs with high aspect ratios (AR = 25,000 for 200 μm long CNTs with 8 nm diameter), enhancing both charge storage capability and cycling life (**Figure 15**a and b).[70] A very high volumetric capacitance of 84.0 F/cm^3 was obtained which is among the highest values reported for similar systems[155,158,163–165]

In another work by Biloiu et al. an amorphous fluorocarbon polymer film, namely perfluoro-octane grown by plasma enhanced chemical vapor deposition (PECVD) was used as the dielectric material in a conventional capacitor.[166] Because of the potential for wide scale application, these films have attracted significant interest as interlayer dielectrics in microelectronics,[167,168] and electrical insulator in high voltage devices.[169] The dielectric and insulating properties of the films have been assessed by means of capacitance-voltage and current-voltage characteristics. The dielectric constant of the polymer film is compared with that of Tefzel (-[CH_2-CH_2-]$_n$-[CF_2. CH_2]-) and Teflon $(CF_2)_n$ obtained by conventional chemical polymer synthesis. They have reported dielectric constant of 2.4, with low dielectric loss (below 3×10^{-2}), for the investigated frequency range, 120 Hz-1 MHz. These values are comparable with those for Tefzel films obtained by traditional

chemical methods. The iCVD method for coating CNTs conformally with ultra-thin dielectric films has widely been reported (Figure 4c).[48,170]

3. Water and the Water-Energy Nexus

Fresh water is at the core of sustainability due to its essential role in the development of agriculture, industry and health care. In particular, energy production represents one of the largest ground water withdrawers in the US.[5] However, it is worth noting that the ground water withdrawn for energy production is largely used as coolant and thus a large portion (~97.5%) is returned to the corresponding aquifer as warm discharge.[5] In fact, the net water consumption by energy production is merely 3310 million gallons per day (MGD), equivalent to 3.3% of all consumptive use of water in the US.[5] Nevertheless, it is challenging to maintain the recycling water supply to the energy industry, which represents ~39% of US annual water withdrawal. Consequently, fresh water scarcity is impacting energy production adversely, especially for thermoelectric and nuclear power plants. For example, in the Millstone nuclear-power plant in Connecticut one of two reactors was shut down in early August 2012 for two weeks due to the lack of cool, fresh water, which resulted in 255,000 megawatt hours of lost power production worth several million dollars.[171]

Fresh water can be produced by removing salts and marine organisms from seawater, a process termed seawater desalination. However, the cost to produce fresh water via desalination is higher than that for natural fresh water. Reducing energy consumption has been one of the focuses for lowering the cost of desalted water. This codependence of energy and water are often referred to as the 'energy-water nexus', which has garnered much attention in several recent reports.[4,172]

In the following sections, we will address this energy-water nexus in greater technological detail. First, state-of-the-art desalination processes, their corresponding characteristics, limitations and energy consumption will be briefly discussed. Interface engineering plays a pivotal role in reducing energy consumption and increasing desalination efficiency.

3.1. Reverse Osmosis

A major breakthrough for the seawater desalination process occurred in early 1960s with the invention of reverse osmosis (RO) technology. It has become the dominating technology among recently-constructed and future-planned desalination facilities. In a RO process, seawater is pressurized against a semipermeable membrane that selectively allows the transport of water across membrane but retains salts. RO technology has improved drastically since its invention and new designs of membrane modules and stage configurations can bring the energy consumption of a RO process close to the thermodynamic minimum energy of 1.06 kWh/m^3.[172] However, the RO process suffers considerably from fouling, which drives up the energy consumption, reduces salt rejection efficiency and degrades the RO membranes. Fouling originates from the surface properties of the state-of-the-art RO membranes, namely thin-film-composite (TFC) membranes. Biofouling — the attachment of marine microorganisms on the membrane — occurs immediately when a membrane module is installed and has to be tolerated until the flux is reduced to 25% of the initial value.[173] The desalination process has to be interrupted for periodic cleaning, which reduces productivity and shortens the lifetime of the TFC membranes.

The bottleneck of biofouling can be reduced or even prevented by interface engineering. However, the direct surface

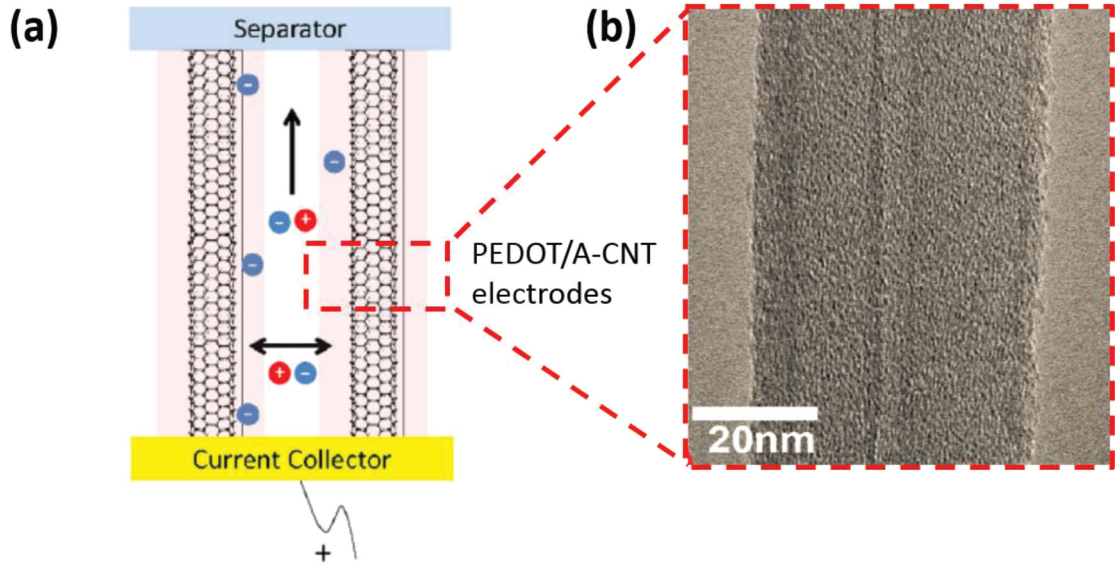

Figure 15. (a) The use of CNTs, conformally coated by oCVD PEDOT, as the electrode of a supercapacitor. (b) TEM image of conformally coated CNTs with oCVD PEDOT are shown.[70] (a,b) Reproduced with permission.[70] Copyright 2014, Elsevier.

modification of commercial TFC membrane is challenging due to its delicate nature. The salt rejection of TFC membranes relies solely on a 100–200 nm thick polyamide layer, which is prone to damage when treated with solvents or at elevated temperature. In addition, the flux of water across membrane decreases rapidly with additional layers of coating. Therefore, an ideal surface modification method should be solvent-free, performed at mild temperature, and should produce ultra-thin (<100 nm) antifouling coatings.

In spite of the challenges, the modification of delicate TFC membranes has been achieved with the benign iCVD process and the resulting membranes resist biofouling very effectively (**Figure 16**a).[66,174,175] The antifouling chemistry applied in these studies is zwitterion, a term referring to molecules with positive and negative charges mixed homogeneously on a molecular level.[176] The strong electrostatic interaction with water makes fouling unfavorable due to the large enthalpic penalty to replace strongly-bound water molecules with microorganisms. Methacrylate-based iCVD zwitterion has demonstrated non-detectable surface attachment from sodium alginate and *Escherichia coli* (*E.coli*) and over 90% reduction in surface protein adsorption.[174,175] The good antifouling behavior was partially attributed to the unique film architecture, with the antifouling zwitterionic moieties concentrated on the uppermost surface.[174] This was achieved by a two-step synthesis scheme, where a precursor film containing tertiary amines was deposited in the first step, and reacted with 1,3-propanesultone under diffusion limitations in the second step.[175]

The long-term stability of the surface-modified membranes was enhanced in two ways. First, covalent chemical bonds were formed to tether the antifouling coating directly to the surface of a commercial membrane.[175] Second, the methacrylate-based zwitterionic structure was later re-designed to resist the oxidative damages by chlorine.[66] The chlorine-resistance enabled an interesting synergistic interaction between surface zwitterionic coating and solution-dissolved hypochlorite, which improved the fouling resistance by 10 times compared to the case where multiplicative effects between chlorination and coating were assumed.[66] Desalination performance of the modified membranes remains unchanged, which indicates that iCVD is able to render membrane surface antifouling without damaging the delicate underlying membrane substrate. iCVD therefore represents one of the most appropriate surface modification methods for the delicate TFC membranes.

Zwitterionic chemistry is only one example in the rich library of antifouling chemistries that is compatible with iCVD.[177–181] Poly(ethylene oxide) (PEO), which is considered the gold standard for antifouling chemistry, has been synthesized using iCVD via a unique ring-opening cationic polymerization mechanism.[177] The PEO brushes were grafted and patterned onto amine-terminated surfaces, and good fouling resistance was evidenced by the sharp contrast of patterns when the surface is subject to bovine serum albumin (BSA) treatment (Figure 16b). Amphiphilic surfaces represent another interesting category of antifouling chemistry. They are smooth surfaces with compositional heterogeneities at a molecular-length scale to disrupt surface–protein interactions.[179] The preparation of such films is challenging because it requires the random copolymerization of hydrophilic and hydrophobic monomers, which have highly contrasting solubility and lack a common solvent. iCVD has successfully synthesized and applied such coatings directly to commercial RO membranes due to its solvent-free nature.[179]

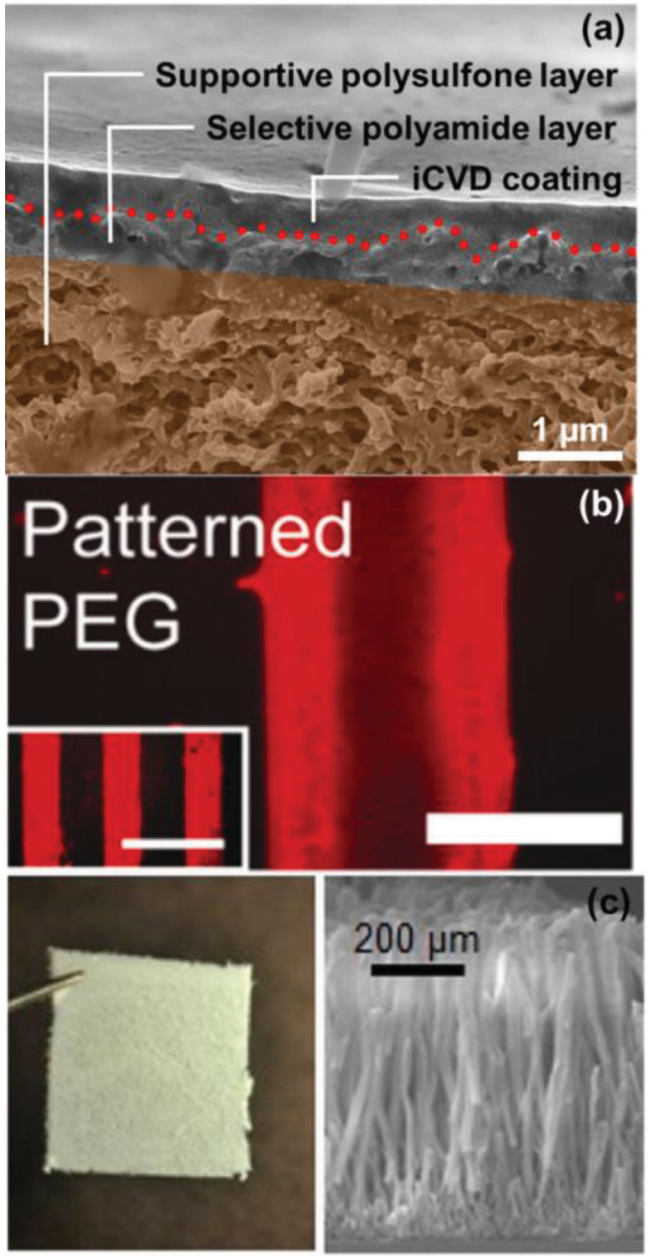

Figure 16. (a) Commercial TFC membranes modified with antifouling coatings via iCVD. The coating adheres well to the underlying membrane substrate without damaging the thin selective polyamide layer.[66] (b) PEG brushes grafted and patterned by iCVD via the ring-opening cationic polymerization mechanism.[177] The patterned surface was subject to BSA treatment, which renders the unmodified stripes fluorescent and PEG-modified stripes dark due to the good fouling resistance of PEG. (c) Free-standing membranes of poly (methacrylic acid-*co*-ethylene glycol diacrylate) with microstructures fabricated in a single step via iCVD.[67] (a) Reproduced with permission.[66] Copyright 2013, Wiley. (b) Reproduced with permission.[177] Copyright 2012 American Chemical Society. (c) Reproduced with permission.[67] Copyright 2013 American Chemical Society.

The modified membranes demonstrated low surface adsorption for a large variety of foulants.[37,179,182,183]

Interestingly, free-standing membranes have been fabricated with iCVD recently (Figure 16c),[67] which promises to modify the surface morphology and chemistry simultaneously, or even enable the one-pot fabrication of antifouling and high-flux next-generation RO membranes.

3.2. Membrane Distillation

Membrane distillation (MD) is a separation process, used in water desalination, wherein the volatile species in a solution is evaporated and transported through a hydrophobic and micro-porous membrane, driven by the partial pressure difference resulting from temperature difference between the feed and permeate side. MD process has many attractive features including but not limited to low operating temperature and pressure,[184] ability to utilize sustainable and alternative energy sources,[185] and excellent salt rejection factor.[184] So far, most MD studies focus on theoretical modeling of transport process in MD and experimental studies on effects of MD operating condition. In most of these studies, commercial hydrophobic membrane fabricated from polytetrafluoroethylene (PTFE), polypropylene (PP), or polyvinylidenedifluoride (PVDF) have been used without further processing. Few studies have attempted to design and synthesize membranes,[186] and even fewer have exploited surface modification of membranes in vapor phase. Kong et al. and Wu et al. modified hydrophilic cellulose nitrate membranes by plasma polymerizations of octafluorocyclobutane (OFCB) and vinyltrimethylsilicon (VTMS)/carbon tetrafluoride (CF_4) respectively.[187,188] Most plasma polymer layers were deposited on the two surfaces of membranes in the form of globular polymer agglomerates, shown in **Figure 17**a and b.[187] The hydrophobicity of fluoropolymer was jeopardized by incorporation of membrane ablation products. Song et al. employed plasma polymerization of fluorosilicone on the outside surface of porous polypropylene hollow fibers, and tested them for MD performance.[189] Silane chemistry was also investigated as a method of vapor phase surface modification for MD membrane.[190,191] 1H, 1H, 2H, 2H-perfluoro decyltriethoxysilane (PFS) and trichloromethylsilane (TCS) were applied as surface modifier for inorganic porous membranes.[191] It was shown that the modified membrane gives sufficiently high hydrophobicity and liquid entry pressure for application in MD.[191]

iCVD has shown great potential for modification of MD membranes. The $-CF_3$ terminated side groups of fluorinated acrylate and methacrylate are completely retained after iCVD polymerization, and form comb-like structure, giving the desired hydrophobicity.[136] Microporous membrane formed from electrospun mats have been conformally modified by iCVD of 2-(Perfluorooctyl) ethyl methacrylate) (PFOEMA), and exhibited superhydrophobicity.[193] Recently, iCVD PFDA has been used to fabricate nanoporous membrane for hydrophobicity-based separation (Figure 17c).[192] The pore walls displayed hydrophobicity after iCVD modification, and achieved high selectivity of membrane towards hydrophobic molecules.[192] The hydrophobic membranes for MD require larger pore size, and can be fabricated using similar methodology. Having shown previous successes in synthesizing hydrophobic porous membranes, iCVD exhibits similar promise for MD technology.

3.3. Electrodialysis and Ion Concentration Polarization

Purification of heavily contaminated water is another very important issue, which has broad impact on all aspects of sustainability.[194] Hydraulic fracking, for example, produces large amounts of waste water with extremely high salinity (200,000 ppm, ~5.7 times the salt concentration in seawater), high concentration of suspended solids, heavy metals and radioactive chemicals.[195] The disposal of such waste water creates significant threats to public health, agriculture and the environment. These feed conditions are challenging for currently industrialized solutions for water purification.

Emerging technologies for the treatment of fracking water include electrodialysis (ED)[196] and ion concentration polarization (ICP).[197] These techniques take advantage of the enhanced electrical conductivity of water at higher salinities. Indeed, ICP desalination has demonstrated the ability to operate even under highly contaminated feed conditions,[197] and thus has great potential as a fracking water purification technique. Under these challenging feed conditions, surface modification which allows continuous operation without fouling would provide a clear benefit for the reliable and economic operation of electrical based desalination methods.

The ion-selective membrane is the critical component, which is limiting the development of the electrical based desalination technologies. The current commercial standard membrane is coated with Nafion®, which is impermeable to water and costly, with limited long-term stability. These technological challenges represent opportunities for CVD polymer coatings as hydrophobic fluoropolymers, which are difficult to produce by solution phase methods. In fact, ultra-thin and conformal fluoropolymer coatings have been synthesized successfully with the iCVD technique,[62,198–200] and the small quantity of fluoromonomers required in the iCVD process can reduce the cost of membranes significantly. The good conformality guarantees uniform coverage over porous membrane substrates and durability of the membrane can be increased considerably by enhancing the mechanical strength via cross-linking[200] or by grafting the fluoropolymer covalently to the substrate.[198] A proton exchange membrane has been produced by copolymerizing a fluoro-acrylate (1H, 1H, 2H, 2H,-perfluorodecyl acrylate) and a co-monomer bearing a carboxylic acid moiety (methacrylic acid).[136] The copolymerization of hydrophobic and hydrophilic monomers is enabled by the solvent-free iCVD method. The resulting copolymer has comparable ion conductivity (70 mS/cm) as commercial Nafion®, and is a promising membrane alternative for electrical based desalination methods.

3.4. Thermal Energy Management

Yet another area that illustrates the interplay between energy and water resources is in the management of thermal energy.

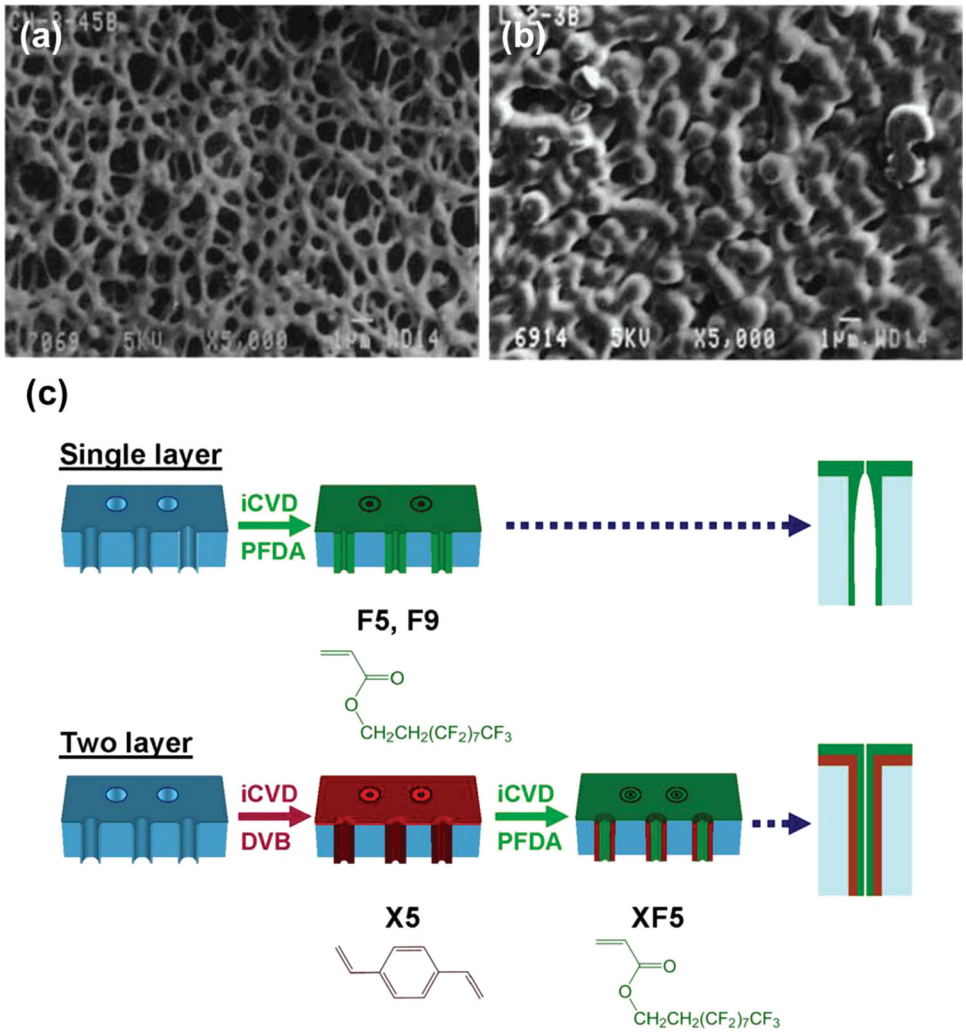

Figure 17. SEM photographs of the (a) surface of base cellulose nitrate membrane and (b) membrane PECVD-modified at 60 min using OFCB (discharge power: 60 W).[187] (c) Single layer membranes (top) are formed in one step by iCVD from PFDA onto track-etched membranes. The pPFDA layer may result in a bottleneck cross section. The bottom shows the two-layer membranes formed by pDVB (red) and pPFDA (green). The resulting narrow cylindrical pore (bottom, right) could be achieved.[192] (a and b) Reproduced with permission.[187] Copyright 1992, Wiley. (c) Reproduced with permission.[192] Copyright 2011, American Chemical Society.

As discussed in this section, thermal management is a fairly broad topic, which can encompass converting heat to electricity or harvesting waste heat generated by other clean energy applications (e.g., PV), or reducing the demand for fresh water as coolant by enhancing heat exchange efficiency in power plants.

3.4.1. Thermoelectric

Thermoelectric (TE) materials have recently attracted significant interest for converting thermal energy to electric energy in the automobile industry, for recapturing energy currently lost from the hot effluent of power plant smokestacks, and for harvesting the heat currently generated, but not used, by photovoltaic cells.[201,202] By understanding how heat and energy flow through materials, energy conversion mechanisms and processes can be integrated into functional devices. A simplified schematic of a thermoelectric device is shown in **Figure 18**a.[203] The two main constituent parts are n and p type materials. These materials are positioned to be electrically in series, but thermally in parallel. In the n-type material, the electrons thermally diffuse to the cold side, while in the p-type material a temperature gradient causes the propagation of holes towards the lower energy region. Therefore, a net charge will be generated due to the build-up of charge carriers diffusing from the hot end to the cold end. The performance of the thermoelectric material is evaluated by the dimensionless figure of merit, *ZT*, that is a function of electrical conductivity, σ, thermal conductivity k, absolute temperature T, and Seebeck coefficient α, defined as the ratio of the induced voltage over the temperature gradient across the thermoelectric device:[202]

$$ZT = \alpha^2 \sigma T/k \quad (1)$$

A general principle for engineering desirable TE materials is to separate electrical from thermal conductivity—in particular, to make them dependent on structures at different length scales.

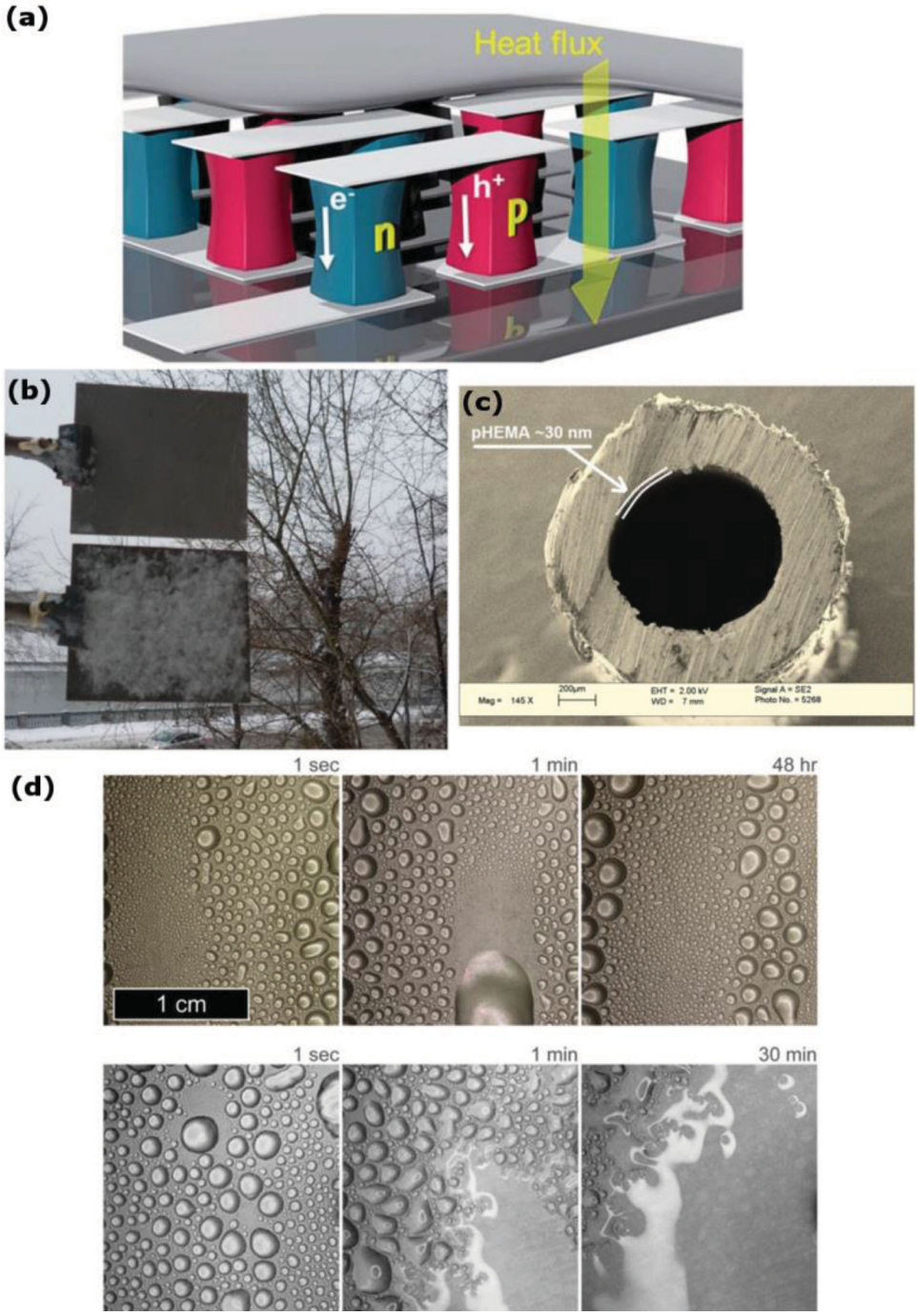

Figure 18. (a) Schematic of thermoelectric device. (b) Icephobic behavior of a superhydrophobic polymer coating (top) and untreated stainless steel (bottom). (c) SEM image on the inner wall of the microtube with polyhydroxyethylmethacrylate (pHEMA) for boiling heat transfer enhancement. (d) Photographs taken during condensation of saturated steam at 100 °C and 101 kPa of prolonged dropwise condensation on grafted coating over a period of 48 hours (top) and degradation of fluorosilane coating over a period of 30 min (bottom).[8] (a) Reproduced with permission.[203] Copyright 2012, The Royal Society of Chemistry. (b) Reproduced with permission.[210] Copyright 2013, American Chemical Society. (c) Reproduced with permission.[211] Copyright 2013, Institute of Physics. (d) Reproduced with permission.[8] Copyright 2013, Wiley.

Today's thermoelectric materials of choice for low temperature energy conversion are bismuth antimony telluride alloys.[204] These constitutive elements are not earth abundant, therefore relatively expensive, and are not environmentally friendly. These factors limit the widespread deployment of these materials in thermoelectric installations for waste heat recovery. In this context, widely available, although less efficient, organic,[203,205] and organic-inorganic thermoelectric nanocomposite[206,207] materials have become the subjects of interest to the scientific community. Different types of polymers as TE materials have been

used in thermoelectric devices, such as polyaniline (PANI), poly(*p*-phenylene vinylene) (PPV), polythiophene (PTH), poly (3, 4-ethylenedioxythiophene): poly(styrenesulfonate) (PEDOT:PSS), polypyrrole (PPY), polycarbazoles (PC), polyacetylene (PA), poly(2,7-carbazolenevinylene), and poly(2,5-dimethoxy phenylenevinylene) (PMeOPV).[203,205,207,208] These polymers are chosen due to their electrically conductive nature. The impact of polymer concentration, molecular weight, chain length, temperature, humidity, and alignment of polymer chain has been studied for TE applications.[205] These polymers have been developed via electro spinning, inkjet printing, and electrochemical deposition.[205,207] It has been recently shown that accurate control of the oxidation level in PEDOT combined with its low intrinsic thermal conductivity ($\lambda = 0.37\ Wm^{-1}K^{-1}$) yields a ZT = 0.25[208] and reducing dopant volume results in ZT = 0.42[209] which approaches the values required for efficient devices.

Oxidative chemical vapor deposition (oCVD) provides conformal PEDOT films without using solvents[30] and might eliminate the need for additional treatments to dope the polymers before integrating them into thermoelectric generators. The conformal, all-dry, substrate-independent, and low-cost characteristics of PEDOT films can potentially be leveraged to make scalable thermoelectric generators on flexible substrates and enable fast processing using roll-to-roll (R2R) systems. The extent of doping and electrical conductivity of such polymers can be tuned throughout the synthesis process by changing growth conditions. In addition, a state-of-the-art mechanism for grafting such polymers to surfaces (Figure 6b) provides the robust adhesion required for industrial application.[40] Through better understanding of transport in amorphous and disordered polymers, it is thus possible to tailor their thermal and electrical conductivity and integrate them into low-cost, scalable, and environmentally-friendly organic thermoelectric generators.

3.4.2. Icephobic Coatings

Ice formation and accumulation can decrease efficiency in energy production in wind turbines[212] and solar photovoltaics,[213] results in mechanical and/or electrical failure in offshore oil platforms,[214] locks and dams,[215] aircrafts,[216] and helicopters,[217] impact monitoring and control in telecommunications equipment,[218] and in general generate safety hazards. Active deicing methods require substantial energy for operation and may have detrimental environmental effects.[219,220] Passive deicing as energy efficient method has recently been employed to protect exposed surfaces using icephobic polymer coatings to inhibit the formation of ice and facilitate the removal of ice deposits (Figure 18b).[210] Good correlation between hydrophobicity of surfaces and their icephobic behavior was previously reported.[221] The initiated chemical vapor deposition (iCVD) method is a promising approach for developing low surface energy fluoropolymers coatings desired for icephobic applications.[62] In addition, iCVD can provide mechanically robust polymer network through incorporation of monomers containing more than one vinyl bond to create cross-linking sites[200] and enables enhanced adhesion of such polymers to desired substrates through grafting techniques.[198]

3.4.3. Heat Transfer Enhancement

Dropwise condensation offers an order of magnitude improvement in heat transfer coefficient when compared to filmwise condensation and can increase efficiency in power generation and desalination processes.[222] Dropwise condensation can be promoted using self-assembled monolayers of oleic acids and deposition of thin film polymers through sputtering or dip-coating. However, these methods for promoting dropwise condensation typically fail due to promoter breakdown, often associated with surface oxidation or difficulties associated with production of sufficiently thin durable surface layers.[223] Thin films of poly-(1*H*,1*H*,2*H*,2*H*-perfluorodecyl acrylate)-*co*-divinyl benzene p(PFDA-*co*-DVB) grafted to metal substrates by iCVD resulted in sustained dropwise condensation of steam when compared to substrates coated with fluorosilane. Figure 18d shows photographs taken during condensation of saturated steam at 100°C and 101 kPa.[8] Heat transfer coefficient in fluorosilane coating (bottom) degrades after 30 minutes and exhibits filmwise condensation while iCVD coating (top) resulted in dropwise condensation even after 48 hours with higher heat transfer coefficient, demonstrating that grafted polymer films deposited via iCVD can generate surfaces with robust dropwise condensation for potential use in heat exchangers.[8] In addition, boiling heat transfer in mini/microtubes was enhanced via iCVD polymerization of hydroxyethylmethacrylate (HEMA) on inner microtube walls for microscale cooling applications.[211] Figure 18c is SEM image on the inner wall of the microtube coated with ~30 nm of pHEMA.

Surface modification using the CVD polymerization techniques discussed here can generate ultra-thin, hydrophobic polymer interfaces on condenser surfaces. This approach if scaled up can potentially improve the efficiency of heat exchange across condensers in both conventional and renewable energy driven power plants, thereby saving hundreds of terawatt hours of energy annually.[8] The resultant energy saving, reduction in CO_2 and improvement of air quality are important metrics for developing a sustainable future.

4. Sensors for Quality of Air, Food, Health

In addition to an abundant supply of clean energy and clean water, sustainable development also requires access to clean air and food along with quality medical care (drugs, diagnostics). Sensing of a wide range of molecular targets such as volatile organic compounds (VOCs), humidity, and biomolecules finds applications in environmental protection, food safety, and human health, respectively.[224] In general, CVD polymers provide a means of synthesizing organic thin films which can be readily integrated with many different types of substrates and sensing devices. For these sensing applications, the desirable attributes of the CVD layers include conformality, substrate independence, mechanically flexibility, and ease of patterning discussed in section 1.2.2.

4.1. Biosensing

Hydrogel films grown from hydroxyethylmethacryate (HEMA) by CVD have been demonstrated to be both conformal and

biocompatible.[10] By varying the degree of incorporation of a crosslinking monomer, such as ethylene glycol diacrylate (EGDA), the mesh size of iCVD hydrogels can be systematically tuned over a size range of ~0.4 to 2.0 nm, which is sufficient to allow the selective passage of small molecule analytes.[225] These properties in combination with film thicknesses ranging from ~10 nm to ~2 μm, have proved useful for encapsulating multiple types of biosensors.

An iCVD-based optode sensor microworm structure enables in vivo measurements of sodium.[9] Its high aspect ratio cylindrical shape (**Figure 19**a) minimizes diffusion away from the point of injection, enabling monitoring to continue over an extended period of time. Additionally, the large surface-area-to-volume ratio of this shape, enhances response time. The fabrication of the microworm sensors begins by conformally coating an iCVD hydrogel layer into the cylindrical pores of an anodized aluminum oxide membrane. Then, an optode solution is filled in the pores of the iCVD coated template and excess optode and hydrogel is etched away. Next, additional iCVD hydrogel layers are deposited on both the top and bottom of the templating membrane to encapsulate the optode. Etching away the membrane releases the microworm sensor.

Low-cost, surface-imprinted polymeric nanotube sensors for the detection of biomolecules like immunoglobulin G (IgG) were demonstrated by Ince et al,[229] following a fabrication scheme related to that for the microworm sensors discussed above. First, the biomolecule IgG was covalently bonded to internal surfaces of a nanoporous membrane. The nanopores, ~100 nm in diameter, were then conformally coated by an ultrathin iCVD hydrogel layer. The low substrate temperature used in iCVD helps avoid degradation of the IgG. After dissolving away the membrane and the IgG, only the iCVD film remained in the form of a forest of molecularly imprinted polymeric nanotubes. The resultant structure displayed selective recognition when exposed to solutions of IgG, confirming that the molecular structure of the biomolecule was preserved in inverse form on the surface of the iCVD nanotubes. A high areal density of binding sites was achieved since the imprinted recognition sites occurred over the entire area of the polymeric iCVD nanotubes, hence overcoming a common limitation of a low density of recognition sites on planar surfaces achieved by molecular imprinting technology utilizing solution applied methods.

Ultrathin pHEMA hydrogel films provide a promising way to protect biosensor electrodes and enhance their response by reducing surface impedance.[230] For microelectrode based biosensors, one factor which limits their response is poor contact at the electrode-electrolyte interface, which will lead to a high impedance and thermal noise. One possible solution is depositing thin films of polymeric hydrogels to reduce the electrode impedance. The pHEMA hydrogel films swelled rapidly and reversibly when exposed to electrolyte solution, with their mesh size remaining small enough to allow permeation of electrolyte while excluding large molecules.

The selective response of organic CVD films can form the basis for biodetection of specific biomolecules, such as food pathogens. As a proof of concept, a biosensor based on the oCVD technique was reported by Bhattacharyya et al.[15] A copolymer of 3,4-ethylenedioxythiophene (EDOT) and 3-thiopheneethanol (3-TE) was conformally deposited on electro-spun

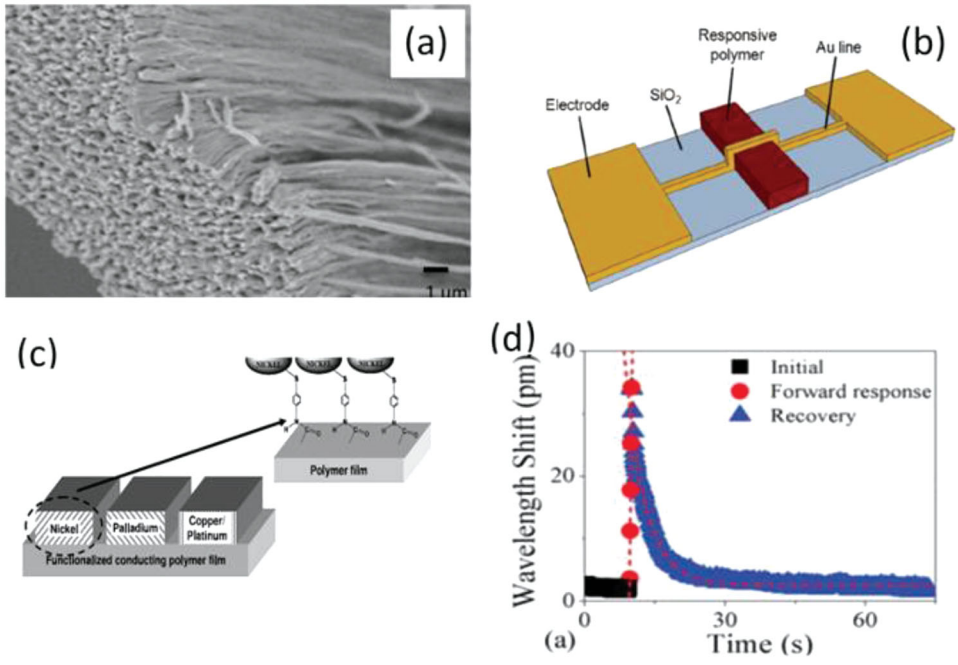

Figure 19. a) SEM images of the microworms.[9] b) Schematic representation of the nitroaromatic organic compounds resistive sensor design.[226] c) Pictorial representation of a multigas/vapor sensor based on a conducting polymer–metal nanoparticle hybrid. Selectivity could be achieved here by varying the metal assembled on top of the same conducting polymer film.[227] d) the sensing response of the hybrid devices with a thin film.[228] a) Reproduced with permission.[9] Copyright 2011, National Academy of Science. b) Reproduced with permission.[226] Copyright 2012, IEEE. c) Reproduced with permission.[227] Copyright 2010, IOP publishing. d) Reproduced with permission.[228] Copyright 2013, AIP Publishing LLC.

mats by oCVD. Using the –OH functionality in the copolymer, the biomolecule avidin was chemically tethered and immobilized on the surface. A uniform distribution of avidin was achieved and the expected selective binding to biotin was demonstrated. A change in electrical resistivity of the avidin-oCVD conducting copolymer films was observed upon exposure to biotin. The high surface area of the nanofiber mats improved the detection limit to concentrations as low as 5 nM of biotin. This chemiresistive response avoids the need to use specifically labeled analytes and large, expensive instrumentation such as lasers and laser detectors. Thus, oCVD resistive food pathogens sensors could be highly portable for widespread use in food safety inspections.

4.2. Chemical Sensing

Chemical sensing is a field drawing increasing attention for applications in environmental protection, security and defense. Integration of polymer CVD films can enable chemiresistive responses, which are highly desirable for small area and lightweight sensors.[231] As reported by Arora et al,[232] a hexylamine sensor was fabricated via integration of reactive polymeric nanofilms into a low power electromechanical switch for selective chemical sensing. Poly[maleic anhydride-alt-di(ethylene glycol)di(vinyl ether)](Poly(Ma-D)) is synthesized using iCVD technique onto a cantilever switch. The polymer covalently reacts with hexylamine, the analyte, and produces a change in stress. As a result, the cantilever deforms and the switch closes and reduces the resistance of the device by over 6 orders of magnitude. The iCVD layer was a robustly adhered ultrathin (75 nm) polymer film, which is of great importance for the stability and response time of this sensor, respectively.

Another important demonstration of iCVD sensors in chemical sensing is selective nitroaromatic (explosives) detection.[16,226] The sensor structure is composed of a stripe of iCVD synthesized poly(4-vinylpyridine)(P4VP) with a metal line lying perpendicular over it (Figure 19b).[226] First, a PMMA template was defined by electron-beam lithography. Above that, a layer of P4VP was deposited with iCVD. After the redundant P4VP was removed with the template, a transverse metal line was patterned using shadow mask and electron beam evaporation. As the P4VP swells specifically when exposed to nitroaromatic compounds, the resistance of the device was permanently changed due to the deformation of polymer and metal line. In the test, the response time is in the order of seconds and detection limit was as low as ~3.7 ppb. In addition to rapid and selective response, the advantages of the iCVD sensor also includes its small area, simplicity and a versatile fabrication scheme, which can be potentially used for producing sensors and sensor arrays targeting a host of other toxic analytes.

In another example demonstrated by Vaddiraju et al.[55,227] a conducting polymer synthesized by oCVD was used in detecting volatile organic compounds (VOCs), which present environmental, health, and safety risks. First, an oCVD copolymer film with –COOH functionality was deposited and then metal nanoparticles were covalently bonded to the surface of the film.[227] When exposed to the VOCs, the work function of the metal nanoparticles changed, and thus the resistance of the hybrid film was changed as well. The detection limitations for toluene and acetone were 2 and 10 ppm, respectively. This chemiresistor based VOC sensor is a readily expandable platform for integration into distributed and wireless sensing systems. The characterizations and the results are shown in Figure 19c. Additionally, peroxide vapors can be sensed by microcantilever sensors, comprising of functional polymer films synthesized by oCVD.[233]

Humidity sensing, as reported by Mehrabani et al,[228] is important for monitoring moisture content in food, which plays an important role in quality control, food storage, and preservation. A nanoscale humidity-responsive polymer coating was deposited by iCVD. The film was integrated into an optical hybrid microcavity humidity sensor and had a sensitivity nearly two orders of magnitude larger compared to conventional refractometric sensing. The polymer film coating on the cavity is poly(N-isopropylacrylamid) (pNIPAAm) deposited by iCVD and the response time decreased with the thickness of film (Figure 19d). The ability of iCVD to grow these uniform and ultra-thin films with 100% functional group reterntion were a key factor in achieving the desired response time and sensitivity (section 1.2.2).

The swelling of pHEMA when exposed to water provides an alternate method to achieve humidity sensing.[14] In a precisely controlled layered hybrid structure, comprising of organic (iCVD pHEMA) and inorganic (hot wire CVD titania) film interfaces, different wavelength of reflectance bands resulted from the Bragg mirror structure. Thus, the color of the hybrid film was affected by the thickness of inner layers. The hybrid heterostructure described above was grown in a single chamber without exposure to atmosphere, providing excellent nanoscale interfacial quality. When exposed to humidity, a change in color from green to red was observed, which changed again to green when a dry nitrogen purge was applied. The rapid (~0.3 sec) and reversible response verified a high optical performance of the structure and its flexibility and simplicity shows potential for such hybrid polymer interfaces to be applied for detection of other analytes.

5. Conclusions and Future Work

In summary, CVD polymerization techniques provide a versatile platform to engineer high quality polymer surfaces and interfaces. In this review, we have given an insight into polymer film growth by the iCVD and oCVD polymerization techniques developed in our laboratory. The high purity films grown by these solvent-free processes do not suffer from surface tension and de-wetting effects, allowing the integration of iCVD and oCVD polymer films onto various substrates, including environmentally friendly substrates like paper. The low-temperature and conformal nature of these vapor based processes further enable the coating of polymer films on substrates with textured surfaces and complex geometries, without damaging them. Facile processing conditions which allow for fast film growth rates (>100 nm/sec), along with the environmentally benign nature of these processes make them amenable for large scale deployment. Film thicknesses can also be precisely controlled over a wide range, along with full retention of surface

functional groups, facilitating the use of these surfaces for sustainable applications in energy, water, air, food, and medicine.

Work on scaling up these economically feasible, high throughput polymer film synthesis processes is currently ongoing both in academic and industrial research labs. When successful, this technology can enable roll-to-roll printing of OPVs and sensors on flexible, stretchable substrates at extremely competitive manufacturing costs. While long-term stability tests on these films are ongoing, several initial promising results have been discussed here for OPVs and heat transfer coatings. Additionally, iCVD grown poly (trivinyltrimethylcyclotrisiloxane) (pV_3D_3) films retained their electrically insulating properties as biopassive coatings for neurally implanted devices even after 2 years of soaking in saline solution.[234] These result show tremendous promise for the integration and stability of iCVD and oCVD grown polymer surfaces in practical applications.

This review also explored ideas for using ultra-thin CVD polymer films as conformal electrolytes in energy storage (e.g., lithium ion batteries), which if successful have the potential to dramatically alter the architecture and performance of these devices. The design of functional polymer film surfaces (e.g., hydrophobic, zwitterion) is yet another feature of CVD polymers that can impact applications in desalination and purification of waste water generated by natural and man-made operations. The water-energy nexus discussed in this review is predicted to become a defining challenge in sustainability, highlighting the imminent need to design approaches that manage both these resources judiciously. One example that is a work in progress, is using polymer CVD coatings for enhancing heat exchange efficiency in power plants, thereby reducing the demand for fresh water as coolant. Not only do these heat exchange coatings promote water conservation, but if deployed on the large scale in power plants, they are estimated to annually save 100s of TWhr of energy, eliminate a billion tons of CO_2 emissions and overall reduce thermal pollution. Furthermore, the amount of raw material usage during the CVD polymerization process is miniscule when compared to the potential savings in energy. Looking forward, these reduced wastage, non-toxic, solvent-free CVD polymerization processes are also promising for designing the next generation of "green" materials, which can one day enable direct integration of electronics with living tissue for applications ranging from diagnostics to drug delivery. The precursors used are earth abundant and do not contain rare, costly elements, and could possibly be derived from natural sources in future. CVD polymerization can thus become an enabling technologies for materials surface and interface modifications that engineer pathways towards a sustainable future.

Acknowledgements

This work was supported by the MIT Institute for Soldier Nanotechnologies (ISN) under Contract DAAD-19–02D-0002 with the U.S. Army Research Office, the King Fahd University of Petroleum and Minerals (KFUPM) in Dhahran, Saudi Arabia, for funding support through the Center for Clean Water and Clean Energy at MIT and KFUPM, and the Masdar Institute. The Office of Naval Research, Office of Naval Research, Advanced Research Projects Agency-Energy, National Science Foundation Scalable Manufacturing and Shell are also kindly acknowledged. C.D.P. gratefully acknowledges support from the National Science Foundation Graduate Research Fellowship Program. R.Y. gratefully acknowledges fellowship from the Wellington and Irene Loh Fund. The authors also gratefully acknowledge Amelia Servi for images of silicon microtrenches.

Received: February 28, 2014
Revised: May 10, 2014
Published online: May 30, 2014

[1] U. Nations, in *Resolution A/66/288*, 27 July **2012**.
[2] J. Bollen, S. Hers, B. van der Zwaan, *Energy Policy* **2010**, *38*, 4021.
[3] M. Z. Jacobson, *Energy Environ. Sci.* **2009**, *2*, 148.
[4] A. Siddiqi, L. D. Anadon, *Energy Policy* **2011**, *39*, 4529.
[5] P. Torcellini, N. Long, R. Judkoff, NREL/CP-550–35190, National Renewable Energy Resources Laboratory **2003**.
[6] *Energy Demands on Water Resources*, United States Department of Energy, **2006**.
[7] S. H. Baxamusa, S. G. Im, K. K. Gleason, *Phys. Chem. Chem. Phys.* **2009**, *11*, 5227.
[8] A. T. Paxson, J. L. Yagüe, K. K. Gleason, K. K. Varanasi, *Adv. Mater.* **2014**, *26*, 418.
[9] G. Ozaydin-Ince, J. M. Dubach, K. K. Gleason, H. A. Clark, *Proc. Natl. Acad. Sci.* **2011**, *108*, 2656.
[10] S. H. Baxamusa, L. Montero, J. M. Dubach, H. A. Clark, S. Borros, K. K. Gleason, *Biomacromolecules* **2008**, *9*, 2857.
[11] K. K. S. Lau, K. K. Gleason, *Surf. Coat. Technol.* **2007**, *201*, 9189.
[12] R. K. Bose, A. M. Heming, K. K. S. Lau, *Macromol. Rapid Commun.* **2012**, *33*, 1375.
[13] G. Yoo, Y. Yoo, J. H. Kwon, C. Darpito, S. K. Mishra, K. Pak, M. S. Park, S. G. Im, J. W. Yang, *Green Chem.* **2014**, *16*, 312.
[14] M. Karaman, S. E. Kooi, K. K. Gleason, *Chem. Mater.* **2008**, *20*, 2262.
[15] D. Bhattacharyya, K. Senecal, P. Marek, A. Senecal, K. K. Gleason, *Adv. Funct. Mater.* **2011**, *21*, 4328.
[16] W. E. Tenhaeff, L. D. McIntosh, K. K. Gleason, *Adv. Funct. Mater.* **2010**, *20*, 1144.
[17] M. E. Alf, A. Asatekin, M. C. Barr, S. H. Baxamusa, H. Chelawat, G. Ozaydin-Ince, C. D. Petruczok, R. Sreenivasan, W. E. Tenhaeff, N. J. Trujillo, S. Vaddiraju, J. Xu, K. K. Gleason, *Adv. Mater.* **2010**, *22*, 1993.
[18] M. Szwarc, *Discussions of the Faraday Society* **1947**, *2*, 46.
[19] W. F. Gorham, *J. Polym. Sci., Part A: Polym. Chem.* **1966**, *4*, 3027.
[20] J. B. Fortin, T.-M. Lu, *Chemical Vapor Deposition Polymerization - The Growth and Properties of Parylene Thin Films*, Kluwer Academic Publishers, Norwell, MA, USA, **2004**.
[21] H.-Y. Chen, J. Lahann, *Langmuir* **2010**, *27*, 34.
[22] A. Kubono, N. Okui, *Prog. Polym. Sci.* **1994**, *19*, 389.
[23] Y.-C. Chang, C. W. Frank, *Langmuir* **1998**, *14*, 326.
[24] H. Zhou, S. F. Bent, *J. Vac. Sci. Technol., A* **2013**, *31*, 040801.
[25] F. F. Shi, *Surf. Coat. Technol.* **1996**, *82*, 1.
[26] M. C. Vasudev, K. D. Anderson, T. J. Bunning, V. V. Tsukruk, R. R. Naik, *ACS Appl. Mater. Interfaces* **2013**, *5*, 3983.
[27] J. Xu, K. K. Gleason, *Chem. Mater.* **2010**, *22*, 1732.
[28] K. K. S. Lau, K. K. Gleason, *Macromolecules* **2006**, *39*, 3688.
[29] K. K. S. Lau, K. K. Gleason, *Macromolecules* **2006**, *39*, 3695.
[30] S. G. Im, K. K. Gleason, *Macromolecules* **2007**, *40*, 6552.
[31] B. Winther-Jensen, K. West, *Macromolecules* **2004**, *37*, 4538.
[32] A. M. Coclite, R. M. Howden, D. C. Borrelli, C. D. Petruczok, R. Yang, J. L. Yagüe, A. Ugur, N. Chen, S. Lee, W. J. Jo, A. Liu, X. Wang, K. K. Gleason, *Adv. Mater.* **2013**, *25*, 5392.
[33] N. J. Trujillo, S. H. Baxamusa, K. K. Gleason, *Chem. Mater.* **2009**, *21*, 742.

[34] V. Georges, H. Kazmeier, *Macromolecules* **1993**, *26*, 5316.
[35] G. Ozaydin-Ince, A. M. Coclite, K. K. Gleason, *Rep. Prog. Phys.* **2012**, *75*, 016501.
[36] K. Chan, K. K. Gleason, *Macromolecules* **2006**, *39*, 3890.
[37] G. Ozaydin-Ince, A. Matin, Z. Khan, S. M. J. Zaidi, K. K. Gleason, *Thin Solid Films* **2013**, *539*, 181.
[38] R. Tao, M. Anthamatten, *Langmuir* **2012**, *28*, 16580.
[39] S. H. Baxamusa, L. Montero, S. Borrós, K. K. Gleason, *Macromol. Rapid Commun.* **2010**, *31*, 735.
[40] N. J. Trujillo, M. C. Barr, S. G. Im, K. K. Gleason, *J. Mater. Chem.* **2010**, *20*, 3968.
[41] R. Sreenivasan, K. K. Gleason, *Chem. Vap. Deposition* **2009**, *15*, 77.
[42] N. Gospodinova, L. Terlemezyan, *Prog. Polym. Sci.* **1998**, *23*, 1443.
[43] D. Bhattacharyya, R. M. Howden, D. C. Borrelli, K. K. Gleason, *Journal of Polymer Science Part B: Polymer Physics* **2012**, *50*, 1329.
[44] R. M. Howden, E. D. McVay, K. K. Gleason, *J. Mater. Chem. A* **2013**, *1*, 1334.
[45] H. Park, R. M. Howden, M. C. Barr, V. Bulović, K. Gleason, J. Kong, *ACS Nano* **2012**, *6*, 6370.
[46] G. Ozaydin-Ince, K. K. Gleason, *J. Vac. Sci. Technol., Surfaces, and Films* **2009**, *27*, 1135.
[47] S. H. Baxamusa, K. K. Gleason, *Chem. Vap. Deposition* **2008**, *14*, 313.
[48] Y. Ye, Y. Mao, H. Wang, Z. Ren, *J. Mater. Chem.* **2012**, *22*, 2449.
[49] M. M. Hassan, J. R. McLaughlin, *ACS Appl. Mater. Interfaces* **2013**, *5*, 1548.
[50] S. G. Im, D. Kusters, W. Choi, S. H. Baxamusa, M. C. M. van de Sanden, K. K. Gleason, *ACS Nano* **2008**, *2*, 1959.
[51] Y. Yoo, J. B. You, W. Choi, S. G. Im, *Polym. Chem.* **2013**, *4*, 1664.
[52] E. D. Laird, R. K. Bose, W. Wang, K. K. Lau, C. Y. Li, *Macromol. Rapid Commun.* **2013**, *34*, 251.
[53] P. D. Haller, L. C. Bradley, M. Gupta, *Langmuir* **2013**, *29*, 11640.
[54] R. J. Frank-Finney, L. C. Bradley, M. Gupta, *Macromolecules* **2013**, *46*, 6852.
[55] S. Vaddiraju, K. Seneca, K. K. Gleason, *Adv. Funct. Mater.* **2008**, *18*, 1929.
[56] S. G. Im, B. S. Kim, L. H. Lee, W. E. Tenhaeff, P. T. Hammond, K. K. Gleason, *Macromol. Rapid Commun.* **2008**, *29*, 1648.
[57] N. Marí-Buyé, S. O'Shaughnessy, C. Colominas, C. E. Semino, K. K. Gleason, S. Borros, *Adv. Funct. Mater.* **2009**, *19*, 1276.
[58] T. P. Martin, K. L. Sedransk, K. Chan, S. H. Baxamusa, K. K. Gleason, *Macromolecules* **2007**, *40*, 4586.
[59] W. E. Tenhaeff, K. K. Gleason, *Adv. Funct. Mater.* **2008**, *18*, 979.
[60] S. G. Im, P. J. Yoo, P. T. Hammond, K. K. Gleason, *Adv. Mater.* **2007**, *19*, 2863.
[61] R. Yang, T. Buonassisi, K. K. Gleason, *Adv. Mater.* **2013**, *25*, 2078.
[62] A. M. Coclite, Y. Shi, K. K. Gleason, *Adv. Funct. Mater.* **2012**, *22*, 2167.
[63] M. C. Barr, J. A. Rowehl, R. R. Lunt, J. J. Xu, A. N. Wang, C. M. Boyce, S. G. Im, V. Bulovic, K. K. Gleason, *Adv. Mater.* **2011**, *23*, 3500.
[64] M. C. Barr, C. Carbonera, R. Po, V. Bulovic, K. K. Gleason, *Appl. Phys. Lett.* **2012**, *100*, 183301.
[65] M. C. Barr, R. M. Howden, R. R. Lunt, V. Bulovic, K. K. Gleason, *Adv. Energy Mater.* **2012**, *2*, 1404.
[66] R. Yang, H. Jang, R. Stocker, K. K. Gleason, *Adv. Mater.* **2014**, *26*, 1711.
[67] S. Seidel, P. Kwong, M. Gupta, *Macromolecules* **2013**, *46*, 2976.
[68] S. Nejati, K. K. S. Lau, *Nano Lett.* **2011**, *11*, 419.
[69] T. S. Arthur, D. J. Bates, N. Cirigliano, D. C. Johnson, P. Malati, J. M. Mosby, E. Perre, M. T. Rawls, A. L. Prieto, B. Dunn, *MRS Bulletin* **2011**, *36*, 523.
[70] M. Ghaffari, S. Kosolwattana, Y. Zhou, N. Lachman, M. Lin, D. Bhattacharya, K. K. Gleason, B. L. Wardle, Q. M. Zhang, *Electrochim. Acta* **2013**, *112*, 522.
[71] M. Gupta, K. K. Gleason, *Thin Solid Films* **2006**, *515*, 1579.
[72] K. L. Choy, *Prog. Mater. Sci.* **2003**, *48*, 57.
[73] X.-T. Yan, Y. Xu, in *Chemical Vapour Deposition*, Springer, London, **2010**.
[74] D. Dobkin, M. K. Zuraw, *Principles of Chemical Vapor Deposition*, Springer, **2003**.
[75] Y. Pauleau, *Chemical Physics of Thin Film Deposition Processes for Micro- and Nano-Technologies*, Springer, **2002**.
[76] C. R. Kleijn, R. Dorsman, K. J. Kuijlaars, M. Okkerse, H. van Santen, *J. Cryst. Growth* **2007**, *303*, 362.
[77] H. G. P. Lewis, N. P. Bansal, A. J. White, E. S. Handy, *Thin Solid Films* **2009**, *517*, 3551.
[78] A. C. Jones, M. L. Hitchman, *Chemical Vapour Deposition: Precursors, Processes and Applications*, Royal Society of Chemistry, **2009**.
[79] U. Mann, *Principles of Chemical Reactor Analysis and Design: New Tools for Industrial Chemical Reactor Operations*, Wiley, **2009**.
[80] http://www.gvdcorp.com/.
[81] http://www.p2i.com/.
[82] http://www.semblant.com/.
[83] http://www.hzo.com/.
[84] https://www.youtube.com/watch?v = Ln0daAowdJI.
[85] REN21, Paris 2013.
[86] M. Z. Liu, M. B. Johnston, H. J. Snaith, *Nature* **2013**, *501*, 395.
[87] http://www.heliatek.com, 2013.
[88] K. Ellmer, *Nat Photonics* **2012**, *6*, 808.
[89] A. Elschner, S. Kirchmeyer, W. Lovenich, U. Merker, K. Reuter, *PEDOT: Principles and Applications of an Intrinsically Conductive Polymer,* CRC Press, **2010**.
[90] J. Y. Ouyang, *ACS Appl. Mater. Interfaces* **2013**, *5*, 13082.
[91] M. V. Fabretto, D. R. Evans, M. Mueller, K. Zuber, P. Hojati-Talemi, R. D. Short, G. G. Wallace, P. J. Murphy, *Chem. Mater.* **2012**, *24*, 3998.
[92] Y. J. Xia, K. Sun, J. Y. Ouyang, *Adv. Mater.* **2012**, *24*, 2436.
[93] H. Chelawat, S. Vaddiraju, K. Gleason, *Chem. Mater.* **2010**, *22*, 2864.
[94] T. Bashir, M. Skrifvars, N. K. Persson, *Polym Advan Technol* **2011**, *22*, 2214.
[95] T. Bashir, L. Fast, M. Skrifvars, N. K. Persson, *J. Appl. Polym. Sci.* **2012**, *124*, 2954.
[96] T. Bashir, M. Skrifvars, N. K. Persson, *Polym Advan Technol* **2012**, *23*, 611.
[97] R. M. Howden, E. J. Flores, V. Bulovic, K. K. Gleason, *Org Electron* **2013**, *14*, 2257.
[98] J. Yin, J. L. Yague, D. Eggenspieler, K. K. Gleason, M. C. Boyce, *Adv. Mater.* **2012**, *24*, 5441.
[99] S. Nejati, K. K. S. Lau, *Langmuir* **2011**, *27*, 15223.
[100] G. Li, R. Zhu, Y. Yang, *Nat Photonics* **2012**, *6*, 153.
[101] A. Polman, H. A. Atwater, *Nat Mater* **2012**, *11*, 174.
[102] J. B. Kim, P. Kim, N. C. Pegard, S. J. Oh, C. R. Kagan, J. W. Fleischer, H. A. Stone, Y. L. Loo, *Nat Photonics* **2012**, *6*, 327.
[103] L. Y. Bian, E. W. Zhu, J. Tang, W. H. Tang, F. J. Zhang, *Prog. Polym. Sci.* **2012**, *37*, 1292.
[104] D. C. Borrelli, M. C. Barr, V. Bulovic, K. K. Gleason, *Sol. Energy Mater. Sol. Cells* **2012**, *99*, 190.
[105] D. Bhattacharyya, K. K. Gleason, *J. Mater. Chem.* **2012**, *22*, 405.
[106] D. C. Borrelli, K. K. Gleason, *Macromolecules* **2013**, *46*, 6169.
[107] A. M. Coclite, G. Ozaydin-Ince, F. Palumbo, A. Milella, K. K. Gleason, *Plasma Process Polym* **2010**, *7*, 561.
[108] D. A. Spee, M. R. Schipper, C. H. M. van der Werf, J. K. Rath, R. E. I. Schropp, *Thin Solid Films* **2013**, *532*, 84.
[109] A. M. Coclite, G. Ozaydin-Ince, R. d'Agostino, K. K. Gleason, *Macromolecules* **2009**, *42*, 8138.
[110] A. Maria Coclite, F. De Luca, K. K. Gleason, *J. Vac. Sci. Technol., A* **2012**, *30*, 061502-1.
[111] A. M. Coclite, K. K. Gleason, *Plasma Process Polym* **2012**, *9*, 425.

[112] A. M. Coclite, K. K. Gleason, *J. Appl. Phys.* **2012**, *111*, 073516.
[113] G. Aresta, J. Palmans, M. C. M. van de Sanden, M. Creatore, *J. Vac. Sci. Technol., A* **2012**, *30*, 01A131.
[114] G. Aresta, J. Palmans, M. C. M. van de Sanden, M. Creatore, *Microporous Mesoporous Mater.* **2012**, *151*, 434.
[115] Y. S. Li, C. H. Tsai, S. H. Kao, I. W. Wu, J. Z. Chen, C. I. Wu, C. F. Lin, I. C. Cheng, *J Phys D Appl Phys* **2013**, *46*, 435502.
[116] B. O'Regan, M. Grätzel, *Nature* **1991**, *353*, 737.
[117] J. Burschka, N. Pellet, S. J. Moon, R. Humphry-Baker, P. Gao, M. K. Nazeeruddin, M. Grätzel, *Nature* **2013**, *499*, 316.
[118] P. M. Sirimanne, B. Winther-Jensen, H. C. Weerasinghe, Y.-B. Cheng, *Thin Solid Films* **2010**, *518*, 2871.
[119] A. J. Mozer, D. K. Panda, S. Gambhir, T. C. Romeo, B. Winther-Jensen, G. G. Wallace, *Langmuir* **2010**, *26*, 1452.
[120] J. Xia, L. Chen, S. Yanagida, *J. Mater. Chem.* **2011**, *21*, 4644.
[121] X. Li, W. Lu, W. Dong, Q. Chen, D. Wu, W. Zhou, L. Chen, *Nanoscale* **2013**, *5*, 5257.
[122] J. Chen, P. Wagner, L. Tong, D. Boskovic, W. Zhang, D. Officer, G. G. Wallace, G. F. Swiegers, *Chem. Sci.* **2013**, *4*, 2797.
[123] B. Winther-Jensen, D. R. MacFarlane, *Energy Environ. Sci.* **2011**, *4*, 2790.
[124] B. Winther-Jensen, K. Fraser, C. Ong, M. Forsyth, D. R. MacFarlane, *Adv. Mater.* **2010**, *22*, 1727.
[125] S. Roualdès, M. Schieda, L. Durivault, I. Guesmi, E. Gérardin, J. Durand, *Chem. Vap. Deposition* **2007**, *13*, 361.
[126] R. Kerr, C. Pozo-Gonzalo, M. Forsyth, B. Winther-Jensen, *ECS Electrochem. Lett.* **2013**, *2*, F29.
[127] H. Mahdjoub, S. Roualdès, P. Sistat, N. Pradeilles, J. Durand, G. Pourcelly, *Fuel Cells* **2005**, *5*, 277.
[128] P. D. Beattie, F. P. Orfino, V. I. Basura, K. Zychowska, J. Ding, C. Chuy, J. Schmeisser, S. Holdcroft, *J. Electroanal. Chem.* **2001**, *503*, 45.
[129] F. Finsterwalder, G. Hambitzer, *J. Membr. Sci.* **2001**, *185*, 105.
[130] Z. Jiang, Z.-j. Jiang, Y. Meng, *J. Membr. Sci.* **2011**, *372*, 303.
[131] A. Ennajdaoui, S. Roualdes, P. Brault, J. Durand, *J. Power Sources* **2010**, *195*, 232.
[132] S. Roualdes, I. Topala, H. Mahdjoub, V. Rouessac, P. Sistat, J. Durand, *J. Power Sources* **2006**, *158*, 1270.
[133] J. Thery, S. Martin, V. Faucheux, L. Le Van Jodin, D. Truffier-Boutry, A. Martinent, J. Y. Laurent, *J. Power Sources* **2010**, *195*, 5573.
[134] C. Zhang, J. Hu, X. Wang, H. Toyoda, M. Nagatsu, X. Zhang, Y. Meng, *J. Power Sources* **2012**, *198*, 112.
[135] Y. Uchimoto, K. Yasuda, Z. Ogumi, Z.-i. Takehara, *J. Electrochem. Soc.* **1991**, *138*, 3190.
[136] A. M. Coclite, P. Lund, R. Di Mundo, F. Palumbo, *Polymer* **2013**, *54*, 24.
[137] Z. Jiang, Z.-j. Jiang, *RSC Adv.* **2012**, *2*, 2743.
[138] Z. Jiang, Z.-j. Jiang, X. Yu, Y. Meng, *Plasma Process Polym* **2010**, *7*, 382.
[139] B. Winther-Jensen, O. Winther-Jensen, M. Forsyth, D. R. MacFarlane, *Science* **2008**, *321*, 671.
[140] P. P. Cottis, D. Evans, M. Fabretto, S. Pering, P. Murphy, P. Hojati-Talemi, *RSC Adv.* **2014**, *4*, 9819.
[141] S. G. Kandalkar, D. S. Dhawale, C. K. Kim, C. D. Lokhande, *Synthetic Metals* **2010**, *160*, 1299.
[142] C. Largeot, C. Portet, J. Chmiola, P. L. Taberna, Y. Gogotsi, P. Simon, *J. Am. Chem. Soc.* **2008**, *130*, 2730.
[143] P. Simon, Y. Gogotsi, *Nat Mater* **2008**, *7*, 845.
[144] M. S. Wu, P. C. J. Chiang, *Electrochem Solid St* **2004**, *7*, A123.
[145] X. P. Dong, W. H. Shen, J. L. Gu, L. M. Xiong, Y. F. Zhu, Z. Li, J. L. Shi, *J Phys Chem B* **2006**, *110*, 6015.
[146] W. Sugimoto, H. Iwata, Y. Murakami, Y. Takasu, *J. Electrochem. Soc.* **2004**, *151*, A1181.
[147] S. B. W. A. Schalkwijk, *Advances in Lithium-Ion Batteries*, Kluwer Academic Publications, New York **2002**.
[148] S. Hirotaka, C. W. Berry, B. E. Casey, G. Lavella, Y. Ying, J. M. Vanden Brooks, M. M. Maharbiz, *MEMS, Tucson, AZ, USA* **2008**, 164.
[149] D. F. Lemmerhirt, K. D. Wise, *Proc. IEEE* **2006**, *94*, 1138.
[150] P. Mohseni, K. Najafi, S. J. Eliades, X. Wang, *IEEE Trans. Neural Syst. Rehab. Eng.* **2005**, *13*, 263.
[151] S. R. Gowda, A. L. M. Reddy, M. M. Shaijumon, X. Zhan, L. Ci, P. M. Ajayan, *Nano Lett.* **2011**, *11*, 101.
[152] D. R. Rolison, J. W. Long, J. C. Lytle, A. E. Fischer, C. P. Rhodes, T. M. McEvoy, M. E. Bourg, A. M. Lubers, *Chem. Soc. Rev.* **2009**, *38*, 226.
[153] K. K. S. Lau, K. K. Gleason, *Adv. Mater.* **2006**, *18*, 1972.
[154] B. E. Conway, V. Birss, J. Wojtowicz, *J. Power Sources* **1997**, *66*, 1.
[155] B. E. Conway, *Electrochemical Supercapacitors: Scientific Fundamentals and Technological Applications*, Kluwer academic /Plenum publishers, New York, **1999**.
[156] Q. Cheng, J. Tang, N. Shinya, L.-C. Qin, *J. Power Sources* **2013**, *241*, 423.
[157] A. Bahloul, B. Nessark, E. Briot, H. Groult, A. Mauger, K. Zaghib, C. M. Julien, *J. Power Sources* **2013**, *240*, 267.
[158] Y. Hou, Y. W. Cheng, T. Hobson, J. Liu, *Nano Lett.* **2010**, *10*, 2727.
[159] V. V. N. Obreja, *Physica E: Low-dimensional Systems and Nanostructures* **2008**, *40*, 2596.
[160] E. Frackowiak, F. Béguin, *Carbon* **2001**, *39*, 937.
[161] D. N. Futaba, K. Hata, T. Yamada, T. Hiraoka, Y. Hayamizu, Y. Kakudate, O. Tanaike, H. Hatori, M. Yumura, S. Iijima, *Nat Mater* **2006**, *5*, 987.
[162] A. Izadi-Najafabadi, S. Yasuda, K. Kobashi, T. Yamada, D. N. Futaba, H. Hatori, M. Yumura, S. Iijima, K. Hata, *Adv. Mater.* **2010**, *22*, E235.
[163] E. Frackowiak, V. Khomenko, K. Jurewicz, K. Lota, F. Béguin, *J. Power Sources* **2006**, *153*, 413.
[164] K. Lota, V. Khomenko, E. Frackowiak, *Journal of Physics and Chemistry of Solids* **2004**, *65*, 295.
[165] X. Bai, X. Hu, S. Zhou, J. Yan, C. Sun, P. Chen, L. Li, *Electrochim. Acta* **2013**, *87*, 394.
[166] C. Biloiu, I. A. Biloiu, Y. Sakai, H. Sugawara, A. Ohta, *J. Vac. Sci. Technol., A* **2004**, *22*, 1158.
[167] K. Endo, T. Tatsumi, *Appl. Phys. Lett.* **1996**, *68*, 3656.
[168] A. Weber, *J. Vac. Sci. Technol., A* **1998**, *16*, 2120.
[169] Y. Sakai, *in Gaseous Dielectrics*, Vol. *IX*, Kluwer Academic, New York **2001**.
[170] Y. Ye, Y. Mao, F. Wang, H. Lu, L. Qu, L. Dai, *J. Mater. Chem.* **2011**, *21*, 837.
[171] R. Smith, in *Wall Street Journal*, Lex Fenwick, New York, NY, 10036 **2012**.
[172] M. Elimelech, W. A. Phillip, *Science* **2011**, *333*, 712.
[173] C. Fritzmann, J. Löwenberg, T. Wintgens, T. Melin, *Desalination* **2007**, *216*, 1.
[174] R. Yang, K. K. Gleason, *Langmuir* **2012**, *28*, 12266.
[175] R. Yang, J. Xu, G. Ozaydin-Ince, S. Y. Wong, K. K. Gleason, *Chem. Mater.* **2011**, *23*, 1263.
[176] S. Jiang, Z. Cao, *Adv. Mater.* **2010**, *22*, 920.
[177] R. K. Bose, S. Nejati, D. R. Stufflet, K. K. S. Lau, *Macromolecules* **2012**, *45*, 6915.
[178] Y. Ye, Y. Mao, *J. Mater. Chem.* **2011**, *21*, 7946.
[179] S. H. Baxamusa, K. K. Gleason, *Adv. Funct. Mater.* **2009**, *19*, 3489.
[180] R. K. Bose, K. K. S. Lau, *Biomacromolecules* **2011**, *11*, 2116.
[181] R. Yang, A. Asatekin, K. K. Gleason, *Soft Matter* **2012**, *8*, 31.
[182] A. Matin, Z. Khan, K. K. Gleason, M. Khaled, S. M. J. Zaidi, A. Khalil, P. Moni, R. Yang, *Sep. Purif. Technol.* **2014**, *124*, 117.
[183] A. Matin, H. Z. Shafi, Z. Khan, M. Khaled, R. Yang, K. Gleason, F. Rehman, *Desalination*.
[184] A. Alkhudhiri, N. Darwish, N. Hilal, *Desalination* **2012**, *287*, 2.

[185] J. Blanco Gálvez, L. García-Rodríguez, I. Martín-Mateos, *Desalination* **2009**, *246*, 567.
[186] D. E. Suk, T. Matsuura, H. B. Park, Y. M. Lee, *Desalination* **2010**, *261*, 300.
[187] Y. Kong, X. Lin, Y. Wu, J. Chen, J. Xu, *J. Appl. Polym. Sci.* **1992**, *46*, 191.
[188] Y. L. Wu, Y. Kong, X. Lin, W. H. Liu, J. P. Xu, *J. Membr. Sci.* **1992**, *72*, 189.
[189] L. Song, B. Li, K. K. Sirkar, J. L. Gilron, *Ind. Eng. Chem. Res.* **2007**, *46*, 2307.
[190] S. Krajewski, W. Kujawski, M. Bukowska, C. Picard, A. Larbot, *J. Membr. Sci.* **2006**, *281*, 253.
[191] Z. D. Hendren, J. Brant, M. R. Wiesner, *J. Membr. Sci.* **2009**, *331*, 1.
[192] A. Asatekin, K. K. Gleason, *Nano Lett.* **2011**, *11*, 677.
[193] M. Ma, Y. Mao, M. Gupta, K. K. Gleason, G. C. Rutledge, *Macromolecules* **2005**, *38*, 9742.
[194] R. D. Vidic, S. L. Brantley, J. M. Vandenbossche, D. Yoxtheimer, J. D. Abad, *Science* **2013**, *340*.
[195] R. Hammer, J. VanBriesen, Natural Resources Defense Council, 2012.
[196] T. Xu, C. Huang, *AIChE J.* **2008**, *54*, 3147.
[197] S. J. Kim, S. H. Ko, K. H. Kang, J. Han, *Nat Nano* **2010**, *5*, 297.
[198] A. M. Coclite, Y. Shi, K. K. Gleason, *Adv. Mater.* **2012**, *24*, 4534.
[199] M. Gupta, K. K. Gleason, *Thin Solid Films* **2009**, *517*, 3547.
[200] J. L. Yagüe, K. K. Gleason, *Macromolecules* **2013**, *46*, 6548.
[201] H. Alam, S. Ramakrishna, *Nano Energy* **2013**, *2*, 190.
[202] M. W. Gaultois, T. D. Sparks, C. K. H. Borg, R. Seshadri, W. D. Bonificio, D. R. Clarke, *Chem. Mater.* **2013**, *25*, 2911.
[203] O. Bubnova, X. Crispin, *Energy Environ. Sci.* **2012**, *5*, 9345.
[204] J. Chen, T. Sun, D. Sim, H. Peng, H. Wang, S. Fan, H. H. Hng, J. Ma, F. Y. C. Boey, S. Li, M. K. Samani, G. C. K. Chen, X. Chen, T. Wu, Q. Yan, *Chem. Mater.* **2010**, *22*, 3086.
[205] M. A. Kamarudin, S. R. Sahamir, R. S. Datta, B. D. Long, M. F. M. Sabri, S. M. Said, *Scientific World Journal* **2013**.
[206] K. Chatterjee, A. Suresh, S. Ganguly, K. Kargupta, D. Banerjee, *Materials Characterization* **2009**, *60*, 1597.
[207] Y. Du, S. Z. Shen, K. Cai, P. S. Casey, *Prog. Polym. Sci.* **2012**, *37*, 820.
[208] O. Bubnova, Z. U. Khan, A. Malti, S. Braun, M. Fahlman, M. Berggren, X. Crispin, *Nat Mater* **2011**, *10*, 429.
[209] G. H. Kim, L. Shao, K. Zhang, K. P. Pipe, *Nat Mater* **2013**, *12*, 719.
[210] L. B. Boinovich, A. M. Emelyanenko, V. K. Ivanov, A. S. Pashinin, *ACS Appl. Mater. Interfaces* **2013**, *5*, 2549.
[211] A. Kaya, R. Demiryurek, E. Armagan, G. Ozaydin-Ince, M. Sezen, A. Kosar, *J. Micromech. Microeng.* **2013**, *23*.
[212] N. Dalili, A. Edrisy, R. Carriveau, *Renewable and Sustainable Energy Reviews* **2009**, *13*, 428.
[213] R. W. Andrews, A. Pollard, J. M. Pearce, *Sol. Energy Mater. Sol. Cells* **2013**, *113*, 71.
[214] S. B. Subramanyam, K. Rykaczewski, K. K. Varanasi, *Langmuir* **2013**, *29*, 13414.
[215] S. Frankenstein, A. M. Tuthill, *J. Cold Reg. Eng.* **2002**, *16*, 83.
[216] R. Menini, Z. Ghalmi, M. Farzaneh, *Cold Reg. Sci. Tech.* **2011**, *65*, 65.
[217] P. K. Dutta, C. C. Ryerson, C. Pergantis, in *Materials for Space Applications*, Vol. *851* (Eds: M. Chipara, D. L. Edwards, R. S. Benson, S. Phillips), Materials Research Society, Warrendale **2005**, 563.
[218] H. Saito, K. Takai, H. Takazawa, G. Yamauchi, *Mater. Sci. Res. Int.* **1997**, *3*, 216.
[219] J. X. Lai, C. Liu, C. B. Gong, in *Frontiers of Green Building, Materials and Civil Engineering*, Pts 1–8, Vol. *71–78* (Eds: D. Sun, W. P. Sung, R. Chen), Trans Tech Publications Ltd, Stafa-Zurich **2011**, 1865.
[220] C. Laforte, J. L. Laforte, *J. Adhes. Sci. Technol.* **2012**, *26*, 603.
[221] A. J. Meuler, J. D. Smith, K. K. Varanasi, J. M. Mabry, G. H. McKinley, R. E. Cohen, *ACS Appl. Mater. Interfaces* **2010**, *2*, 3100.
[222] I. Tanasawa, *Recent Advances in Condensation Heat Transfer*, Proceedings of the 10th International Heat Transfer Conference, Brighton, England, **1994**, *1*, 197.
[223] J. W. Rose, *International Communications in Heat and Mass Transfer* **1988**, *15*, 449.
[224] S. Okazaki, H. Nakagawa, S. Asakura, Y. Tomiuchi, N. Tsuji, H. Murayama, M. Washiya, *Sensors and Actuators B: Chemical* **2003**, *93*, 142.
[225] J. L. Yague, K. K. Gleason, *Soft Matter* **2012**, *8*, 2890.
[226] C. D. Petruczok, H. J. Choi, Y. Se Young, A. Asatekin, K. K. Gleason, G. Barbastathis, *J. Microelectromech. Syst.* **2013**, *22*, 54.
[227] S. Vaddiraju, K. K. Gleason, *Nanotechnology* **2010**, *21*, 125503.
[228] S. Mehrabani, P. Kwong, M. Gupta, A. M. Armani, *Appl. Phys. Lett.* **2013**, *102*.
[229] G. O. Ince, E. Armagan, H. Erdogan, F. Buyukserin, L. Uzun, G. Demirel, *ACS Appl. Mater. Interfaces* **2013**, *5*, 6447.
[230] L. Montero, G. Gabriel, A. Guimerà, R. Villa, K. K. Gleason, S. Borrós, *Vacuum* **2012**, *86*, 2102.
[231] E. E. Cantatore, *Springer* **2013**, 154.
[232] W. J. Arora, W. E. Tenhaeff, K. K. Gleason, G. Barbastathis, *J. Microelectromech. Syst.* **2009**, *18*, 97.
[233] J. P. Lock, E. Geraghty, L. C. Kagumba, K. K. Mahmud, *Thin Solid Films* **2009**, *517*, 3584.
[234] W. S. O'Shaughnessy, S. K. Murthy, D. J. Edell, K. K. Gleason, *Biomacromolecules* **2007**, *8*, 2564.